REPUBLIC OF TURKEY

ADANA ALPARSLAN TÜRKEŞ SCIENCE AND TECHNOLOGY UNIVERSITY

FACULTY OF AERONAUTICS

DEPARTMENT OF AEROSPACE ENGINEERING

FRACTURE BEHAVIOR OF 3D PRINTED PLA STRUCTURES

EGE CAN YILDIZ

MASTER OF SCIENCE

ADANA 2022

REPUBLIC OF TURKEY

ADANA ALPARSLAN TÜRKEŞ SCIENCE AND TECHNOLOGY UNIVERSITY

GRADUATE SCHOOL OF NATURAL AND APPLIED SCIENCES

DEPARTMENT OF AEROSPACE ENGINEERING

FRACTURE BEHAVIOR OF 3D PRINTED PLA STRUCTURES

EGE CAN YILDIZ

MASTER OF SCIENCE

SUPERVISOR

ASSOC. PROF. DR. AHMET REFAH TORUN

ADANA 2022

I hereby declare that all information in this thesis has been obtained and presented in accordance with academic rules and ethical conduct. I also declare that, as required by these rules and conduct, I have fully cited and referenced all information that is not original to this work.

[Signature]

Ege Can YILDIZ

ABSTRACT

FRACTURE BEHAVIOR OF 3D PRINTED PLA STRUCTURES

Ege Can YILDIZ

Department of Aerospace Engineering

Supervisor: Assoc. Prof. Dr. Ahmet Refah TORUN

September 2022, XX pages

3D Printing is gaining importance as a cost-efficient, low waste, and flexible manufacturing technology. ABS and PLA filaments are dominating the market as input materials whereas PLA is an advantageous choice thanks to its biodegradable and environmentally friendly properties. 3D printing technology offers various internal structure designs of the produced parts. The thesis aims to determine the effect of internal structure in 3D printing. The results will yield an important contribution in terms of fracture design of 3D printed PLA structures. A total of 44 parts were tested, with different nozzle sizes, filling types, filling ratios, and angles. In this way, the breaking behavior of these PLA products produced in a 3D printer, taking into account many different factors, has been examined in detail. As a result, the effect of nozzle size can be ignored. In addition, the filling ratio affected the brittleness of the part, and the filling type affected the amount of elongation. Stress intensity factors of the parts were calculated using the obtained data.

Keywords: PLA, Green Materials, 3D Print, Fracture Behavior

dedication

ACKNOWLEDGEMENTS

First of all, I cannot hide my excitement when starting my master thesis, which is the biggest step I have taken to complete my postgraduate education.

I would like to express my gratitude to my teacher who always supported me on this path, Assoc. Prof. Dr. Ahmet Refah TORUN. He has shown me the way and never left my questions unanswered. In addition, he has been empathetic and understanding during this difficult period that we have been going through.

And finally, I am happy to dedicate my graduation thesis to my closest friends and my family. It was very important not to let down their support.

Ege Can YILDIZ

Adana, 2022

TABLE OF CONTENTS

LIST OF FIGURES

LIST OF TABLES

NOMENCLATURE

a	crack length
$f_I(a/\omega)$	geometrical factor mode I (tensile)
$f_{II}(a/\omega)$	geometrical factor mode II (shear)
K_I	critical stress intensity factor for mode I (tensile)
K_{II}	critical stress intensity factor for mode II (shear)
P_c	critical fracture load
t	Thickness
ω	Width
α	Angle

1. INTRODUCTION

Polylactic acid mostly known as PLA is a polymer that is formed by sustainable resources. By reason of its characteristic properties, PLA getting universally used in all sections of our lives. Perfectly versatile, %100 percent natural, biodegradable, and can be used in place of petroleum-based products. As a result, PLA is regarded as innoxious, out of danger, and having a significant amount of promise for usage as a green material. Thought to be biodegradable and compostable, the family of aliphatic polyesters accepted as poly (lactic acid) (PLA) is typically based on a-hydroxy acids. Due to concerns about the environment, the economy, and safety, packaging experts and manufacturers have started to partly replace petrochemical-based polymers with environment-friendly ones. Strong competition comes from the thermoplastic, high toughness, high-modulus polymer known as PLA. It can be produced using materials that are yearly renewable, like corn starch and sugar beets. Although there are discussions about the conversion of natural products to PLA, it cannot be ignored that PLA has advanced enough to be implanted in the human body. Its high adaptability enables it to be used in every sector. Even if it is not always the primary choice, its efficiency when applied confirms the reliability of the material.

1.1. Chemical and Mechanical Properties of PLA

Carbon is the primary component of polylactic acid, which explains for its versatility. Chemically, carbon is an element with the symbol C and atomic number 6. It is a tetravalent nonmetal atom that releases four electrons to create covalent chemical connections. Carbon is a common component of all known life due to its abundance, distinctive diversity of organic compounds, and exceptional capacity to form polymers at temperatures experienced on Earth. There are numerous ways in which carbon atoms can connect, giving rise to different allotropes of carbon. With about ten million compounds known to date, carbon creates more compounds than any other element, although the total number of compounds that may theoretically create under normal conditions is much greater [6].

The primary component of PLA and related polymers is carbon. The substance known as polymers is composed of macromolecules, which are extraordinarily massive molecules made

up of several repeating units. Polymers, both manufactured and natural, with a wide range of properties play an important and widespread role in everyday life [7]. Both known man-made substances such as polystyrene and natural biopolymers such as DNA and proteins that are important in biological structure and function are classified as macromolecules. Both natural and synthetic polymers are formed by the polymerization of multiple small molecules known as monomers. Therefore, the following physical properties are different from low-molecular-weight compounds. Toughness, high modulus, viscoelasticity, and tendency to form amorphous and semi-crystalline structures rather than crystalline.

Compared to traditional polymers like polypropylene, polystyrene, and polyurethane, PLA plastic offers good mechanical and chemical qualities.[1] More specifically, in terms of Young's modulus (the capacity to tolerate elongation under stress or compression), tensile strength (the force required to pull something), and flexural strength (the stress required to initiate plastic deformation). Amorphous or semicrystalline structures are typically seen in polymers, which have a significant impact on their mechanical properties. There are always amorphous zones between crystalline sections; polymers, unlike metals, cannot form completely crystalline. PLA's characteristics can be changed from flexible to stiff by varying the quantity of crystalline areas Semicrystalline PLA has an elastic modulus of about 3 GPa, a strain of about 0.04, and a tensile strength of roughly 60 MPa. PLA has this mechanical advantage as a result of its chemical characteristicsIt rapidly alters stereochemistry by polymerizing carefully selected combinations of L or D isomers to allow use in food contact, widely accepted high molecular weight amorphous or It is one of the few polymers that can produce crystalline polymers and is considered safe (GRAS) [2]. PLA can be degraded by direct hydrolysis without the need for an enzyme to catalyze the hydrolysis of ester bonds. To process PLA in large-scale production lines for applications such as injection molding, blow molding, thermoforming, and extrusion, the polymer must have sufficient thermal stability to resist degradation and maintain molecular weight and properties. must be PLA undergoes thermal decomposition at temperatures above 200°C (392°F) through reactions such as hydrolysis, lactide reformation, oxidative backbone scission, and intermolecular or intramolecular transesterification. The degradation rate of PLA is affected by time, temperature, low molecular weight contaminants, and catalyst concentration [3]. PLA homopolymer melts at 175 degrees and has a glass transition temperature of 55 degrees. They need processing temperatures that are generally higher than 190 degrees [4]. These temperatures cause thermal decomposition with opening and chain shear reactions leading to molecular weight loss. This limits the processing range of PLA homopolymers. The

most used method to improve machinability is the inclusion of lactic enantiomers with opposite orientations. Since lactic acid is chiral, it has two enantiomers: L- and D-lactic acid. (Fig 1) L-lactide (PLLA), D-lactide (PDLA), and DL-lactide (PDLLA) are examples of stereoisomers of PLA (Fig 2) [8].

Stereochemistry which deals with the spatial configurations of groups and atoms in a molecule, is also known as the "chemistry of space". The phrase "the isomerism that is caused by non-similar configurations of functional groups or atoms that belong to an atom in space" refers to stereoisomerism. These isomers have identical chemical structures but different atomic configurations. When a chiral molecule or ion has two stereoisomers that are mirror images of one another, these stereoisomers are referred to as enantiomers, and they are frequently identified as being either "right-handed" or "left-handed" based on their absolute configuration or another factor. In chemistry, a molecule or ion is called chiral if it cannot be superimposed over its mirror image using any rotation, translation, or other combination. The two enantiomers have the same chemical properties except that they react with other chiral compounds.

They generally have the same physical properties. Since chirality can be used to describe enantiomers, we can use chiral centers to discover whether a molecule has any enantiomers. So, basically, the main difference between chiral and enantiomers is what they define: chiral describes the atom whereas enantiomers describe the comparison of molecules. In the figure 1 L-D lactic acid enantiomers that we mentioned at the beginning, we can observe the chiral centers to which the carbons are attached.

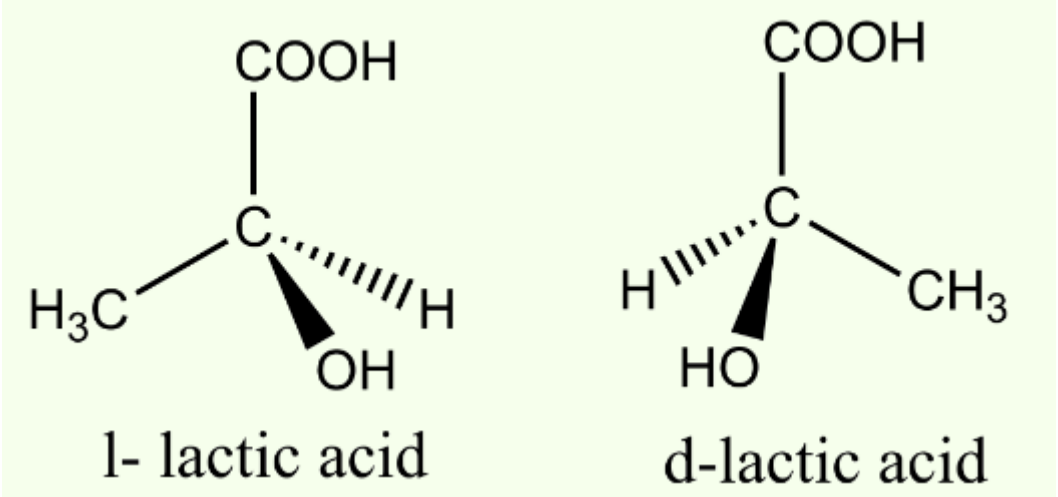

Figure 1 L-D Lactic [70]

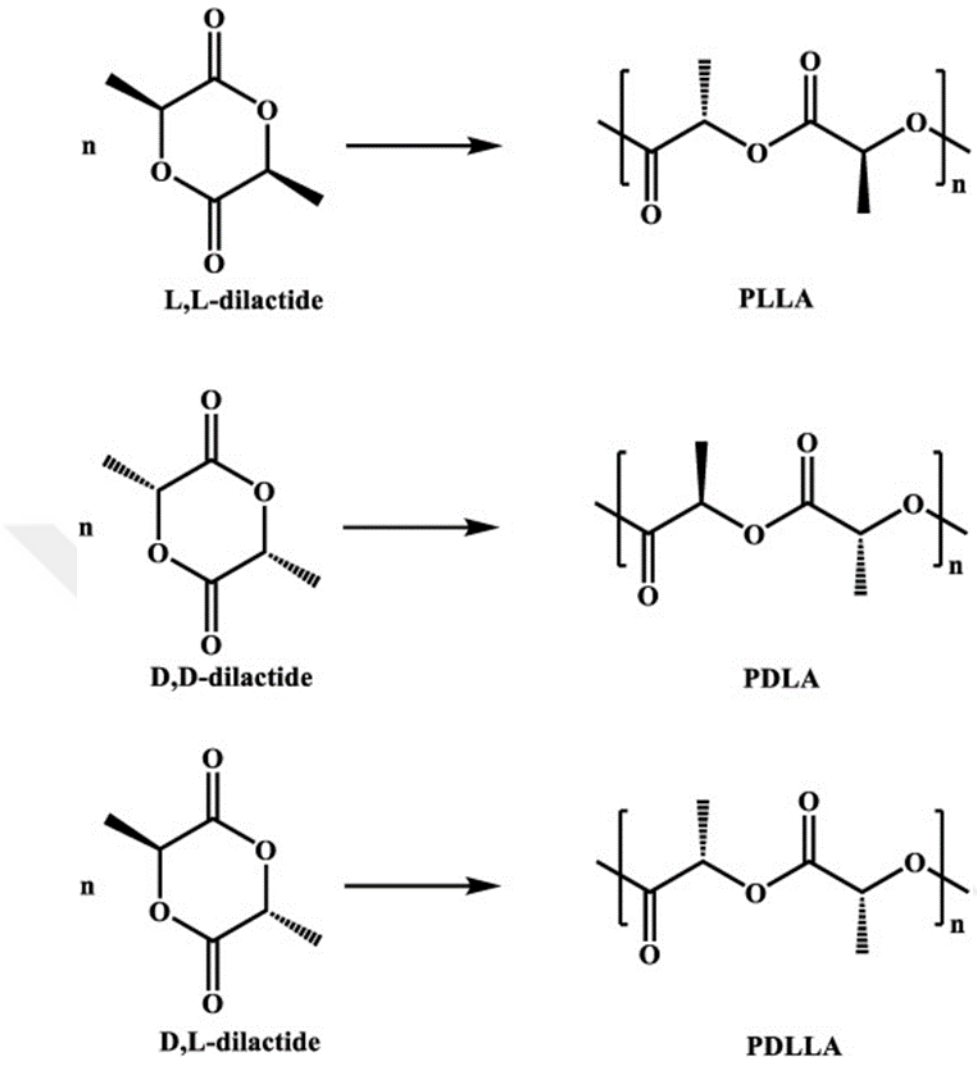

Figure 2 PLLA, PDLA, PDLLA variations [6]

Different enantiomers can be formed in lactic acid because of its asymmetric core. In everyday speech, however, all of these products are referred to as PLA. Nowadays, there are two recognized methods for creating PLA from the monomer lactic acid –polycondensation and ring opening polymerization (ROP). The chemistry of polymerization can be precisely controlled using ROP, and the properties of the resulting polymer can be changed to fit the application. The lactic acid obtained as a result of the fermentation of natural sources can be converted into different types of stereoisomers after distillation. (Table 1) The versatility of PLA is hidden in this chemical chain. Another method is polycondensation, which simply removes small molecules such as water.[5]

Table 1 Stereochemistry of PLA and Their Properties [6]

	L-PLA	Annealed L-PLA	D,L-PLA
Tensile strength (MPa)	59	66	44
Elongation at break (%)	7.0	4.0	5.4
Modulus of elasticity (MPa)	3750	4150	3900
Yield strength (MPa)	70	70	53
Flexural strength (MPa)	106	119	88
Unnotched izod impact (J/m)	195	350	150
Notched izod impact (J/m)	26	66	18
Rockwell hardness	88	88	76
Heat deflection temperature (°C)	55	61	50
Vicat penetration (°C)	59	165	52

1.2. Advantages and Disadvantages

PLA is not only made from renewable resources but it is also recyclable, compostable, and biodegradable. Carbon dioxide is also expelled during manufacturing. The sustainability and environmental friendliness of PLA make it a desirable biopolymer. Thanks to its biocompatibility, it has applications in the field of health, especially in the human body. Thanks to the fact that it does not interact directly with living tissues, PLA can be a common household item or a material that can be inserted into living organisms.

Compared to other biopolymers such as polyhydroxy alkanoates, polyethylene glycol, polycaprolactone, etc., PLA has greater thermal processibility. It can be processed by blow molding, thermoforming, film forming, injection molding, and film extrusion. Unlike petroleum-based polymers, PLA requires 25–55 percent less energy to produce, and predictions indicate that this could eventually fall to less than 10 percent. Production of PLA may be cost-effectively advantageous due to the lower energy consumption. Although excellent biocompatibility, processability, and low energy dependence make PLA a green bioplastic, it also has disadvantages that limit its usage in some situations.

The PLA polymer has a breakage elongation of less than 10%. Its lack of toughness hinders it from being employed in applications that need plastic deformation at greater stress levels, although having the same tensile strength and elastic modulus as poly (ethylene terephthalate) (such as screws and fracture repair plates). Even though PLA plastic is biodegradable, it only breaks down in three months under certain, regulated composting circumstances, i.e., in facilities used for commercial composting. It can take anywhere from 100 to 1000 years to decompose in a landfill. Additionally, there is a basic moral issue with its creation. With the population of the globe increasing, some question if it is moral to use all maize crops, for example, to make bioplastics rather than feed the hungry [9].

1.3. Usage Areas and Sustainability

It is utilized in the packaging, medical, building, textile, and most recently, cosmetics industries. For instance, they are frequently used in furniture, insulating foams, biomedical items, and food storage. The most important reason for the use of PLA in these areas is based on its popularity in 3D printing. Given its price and ease of use, it offers a wide variety for amateurs and professionals alike.

PLA is a sustainable material for the most part. This situation is impacted by production and degrading conditions. It is made from renewable resources that turn CO_2 into glucose by absorbing it. This will next undergo processing to produce a product that contains almost no carbon. However, mixing PLA plastic with other plastics can have an impact on the entire recycling process therefore the proper disposal of PLA plastic calls for extremely precise conditions. Waste PLA plastic must be separated before being delivered to a commercial composting facility. This implies that transportation has an environmental cost. The bioplastic must next be heated to a temperature of nearly 60 °C and exposed to unique bacteria that can degrade the substance.

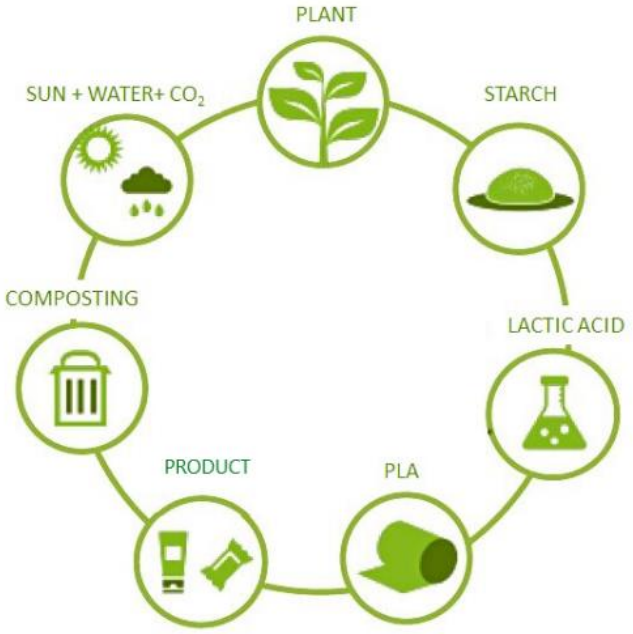

Figure 3 Lifecycle of PLA [69]

Figure 4 Main PLA Application Areas [69]

In Figure 3, we see the transformation of the product, which is actually a plant in our lives, through various changes. It has the quality to continue with the same benefit as long as the life cycle it performs is not disturbed by external factors. Also, can be reused regardless of where it is used as a product.

2. LITERATURE REVIEW

A group of lactide polymers, cyclic dimers formed by dehydration of lactic acid, belong to the family of bioplastics known as polylactic acid or PLA and represent a highly promising and adaptable class of biomaterials. From its inception to its current commercial use, PLA has undergone over 60 years of research and design before becoming an everyday polymer. This overview talks about the development of PLA, its uses, how it degrades, and how it affects the environment. The processing and basic chain features, together with the physical characteristics that have sparked growing interest in PLA, particularly for packaging applications, are also outlined.

I've been trying to collect the universally valid information among thousands of bibliographies describing this journey of PLA from past to present. The information was verified by examining the histories of the people and institutions mentioned in the articles, magazines and books. Although it is difficult to find documents about the information claimed to belong to the pre-1900s, parts of this data adapted to the present have been reached.

2.1. History of PLA

The PLA's beginnings are a subject of intense discussion. The Swedish scientist Carl Wilhelm Scheele's writings are the first well-known sources. In addition to identifying the elements tungsten, hydrogen, barium, and chlorine, Scheele also found oxygen. In the 1770s, the phlogiston hypothesis was the widely accepted theory of gases, which Scheele had learned. He dubbed oxygen, which facilitated combustion, "fire air" when it was first discovered. In his first book, "Chemische Abhandlung von der Luft und dem Feuer," he explained this in German. The first English translation (Chemical Observations and Experiments on Air and Fire), which followed the 1777 publication of the German edition, appeared in 1780. Scheele himself provided an explanation of how milk produces lactic acid, which serves as the basis for PLA. The calcium lactate product referred to as 'Lac Calcis' consists of two lactate anions [10].

The year 1881 is mostly spoken as the date when PLA was first produced commercially. However, there is no document officially confirming this date [11].

The 'Handbook of Stereochemistry', published by the famous German chemist Paul Walden together with Professor Carl Adam Bischof in 1894, confirms this. Walden is well-known for

his contributions to stereochemistry and chemistry history. He created the stereochemical process known as the Walden inversion and created the first ionic liquid to exist at room temperature, ethylammonium nitrate. Walden had to conduct various chemical syntheses and characterizations for the compilation of this manual, leading to the publication of 57 journal publications on stereochemistry alone between 1889 and 1900 in Russian and foreign journals. He persisted with his work in the area of physical chemistry as well, proving in 1889 that the relationship between the dielectric constant and the ionizing power of a non-aqueous solvent is linear. Walden's work on synthesis undoubtedly led to the transition to commercial production [12][13].

The first recorded continuous production of PLA was made in 1932 by Wallace Hume Carothers and his colleagues at Dupont Experimental Station. The development of nylon is attributed to Carothers, an American chemist, inventor, and leader in organic chemistry. He led a team at the DuPont facility, where the majority of polymer research was carried out. Dr. Carothers showed in his studies that he had a high level of originality even at this early stage. He refused to accept the conventional explanations for organic reactions or to take the easy way out. While a student at Harvard, he began to consider polymerization and the structure of materials with large molecular weight. Low molecular weight PLA made by Carothers served as the foundation for DuPont's marketing initiatives in the pharmaceutical and medical industries. DuPont began marketing items for sutures, implants, and drug delivery systems in 1954 [14][15]. In 1954, Dupont Corporation made high molecular weight PLA using improved lactide purification methods and polymerization catalysts such as antimony trioxide and antimony trihalides [16]. Later, techniques for producing high molecular weight PLA with qualities good enough to compete with conventional oil-derived polymers were discovered, but the cost of production made it unaffordable. In the 1960s, researchers studied the crystal structure and configuration of his obtained PLA and its relationship to the chemical structure of the lactide monomer [17]. One of his first polymers used in biomedical applications was he PLA due to its inherent biodegradability. In 1966, Kulkarni et al. We have shown that PLA-based suture materials are absorbed by the human body [18]. Research in the 1970s and 1980s was primarily focused on developing new polymerization catalyst systems, improving their characterization with new analytical techniques, and exploring new medical applications [19]. Recent research has focused on additional catalyst systems, novel copolymers, and polymerization mechanisms in an effort to create more biocompatible polymers. In the early

1990s, techniques for producing lactide and PLA continuously were developed A major step in the commercialization of PLA was taken when Cargill developed technology to manufacture PLA in a continuous process [20][21]. Cargill Dow LLC continues to lead global initiatives to convert annual renewable plants into a variety of useful products such as food wrap materials, films and fibers. Cargill Dow LLC was formed in 1997 as a joint venture between Cargill Incorporated and The Dow Chemical Company. It is a brand-new company whose mission is to create a platform of competitively performing totally renewable, sustainable chemicals and polymers. Utilizing and exploiting a combination of chemical, biological, and agricultural technology is the focus of the company's activities. such as crop cultivation, fermentation, and polymerization. Cargill's Dow just completed polylactide manufacturing facility in Blair, Nebraska increased its annual production capacity of PLA polymer from his 4,000 to 140,000. The facility began operations in November 2001, was producing premium materials by the end of December 2001, and completed the full product manufacturing cycle by February 2002. A nearby polymer plant is accompanied by a 180,000-tonne capacity lactic acid plant built in October 2002. The starch content of corn kernels is converted to dextrose in a nearby corn wet grinder, which Cargill-Dow uses as a raw material for lactic acid fermentation [22].

2.2. Synthesis of PLA

Lactic acid, the main component of PLA, is the most basic hydroxy acid with an extra carbon atom. Two optically active variants are provided. Both the D(-) and L(+) enantiomers are synthesized in bacterial systems, whereas humans and other animals produce only her L(+) isomer. Bacterial fermentation uses lactobacilli to convert cornstarch into lactic acid. Most often, Lactobacillus or one of its modified derivatives ferments lactic acid, which is used commercially around the world. During fermentation, 99.5% L isomer and 0.5% D isomer of lactic acid are formed [23][24]. In a direct condensation approach, lactic acid can be polymerized to PLA using solvent and high vacuum. Alternatively, a solvent-free process produces a cyclic dimer intermediate called lactide, which is then catalyzed to ring-opening polymerization [25]. In polymer chemistry, ring-opening polymerization (ROP) is a type of chain-growth polymerization. To create longer polymers, the ends of the polymer chains attack cyclic monomers. It is conceivable for a reactive center to be radical, cationic, or anionic. Some cyclic monomers, such norbornene or cyclooctadiene, can be polymerized into high molecular weight polymers using metal catalysts. ROP is a versatile method for producing biopolymers. The rings of cyclic monomers typically open when bond-angle strain is reduced. Ring-opening,

like other types of polymerizations, produces a negative enthalpy change as a result. Additionally, radical ROP can be used to create polymers with embedded functional groups that are otherwise impossible to create by regular chain-growth polymerization of vinyl monomers. For instance, radical ROP can create polymers having functional groups throughout the main chain such as ethers, esters, amides, and carbonates [33].

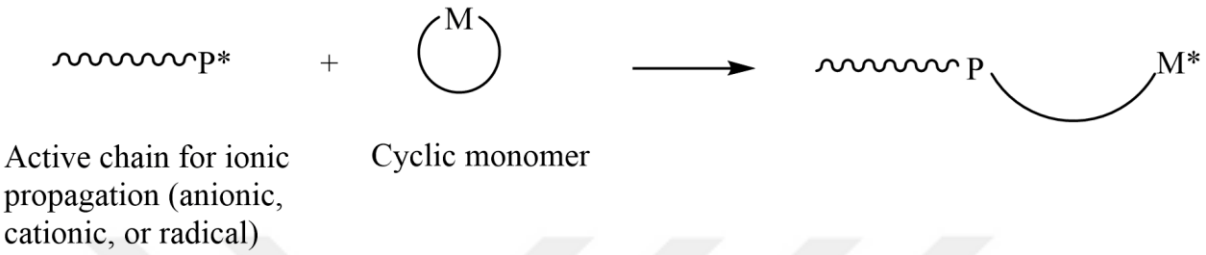

Figure 5 General Scheme of ROP [32]

PLA can also be made by direct condensation of lactic acid monomers. Below 200 °C should be used for this process. Above this point, entropically favored lactide monomers are produced. In this reaction, each condensation (esterification) step produces one equivalent of water. Since the condensation reaction is reversible and equilibrium sensitive, removal of water is required to generate high molecular weight species. To drive the reaction toward polycondensation, water must be removed by applying a vacuum or by azeotropic distillation. In this manner, molecular weights of more than 100 kDa can be obtained. The basic polymer from the melt can be properly crystallized to reach even higher molecular weights [27]. The ROP technique is cheaper than polycondensation, but high molecular weight is difficult to achieve. In Figure 6 we see the ring-opening polymerization of L-D lactides. It is easy to understand that their placement in space is partially symmetrical to each other.

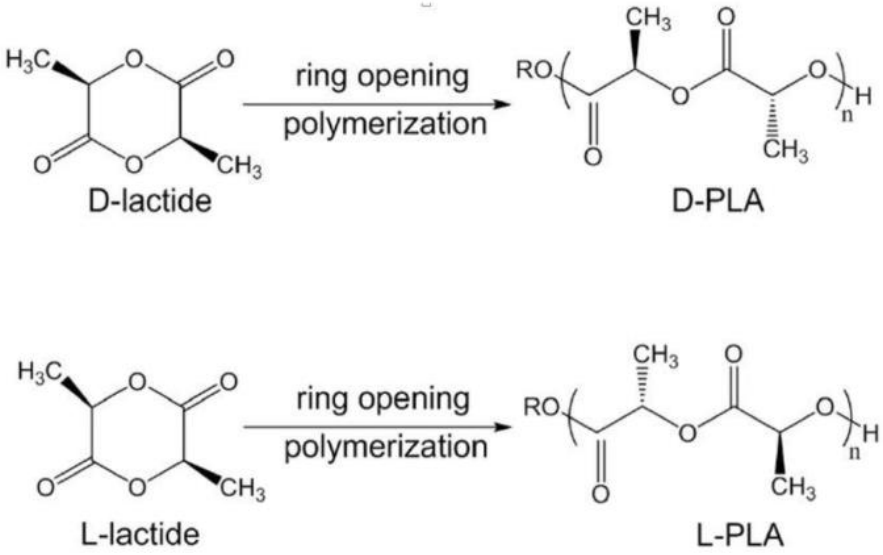

Figure 6 ROP for L and D lactide [31]

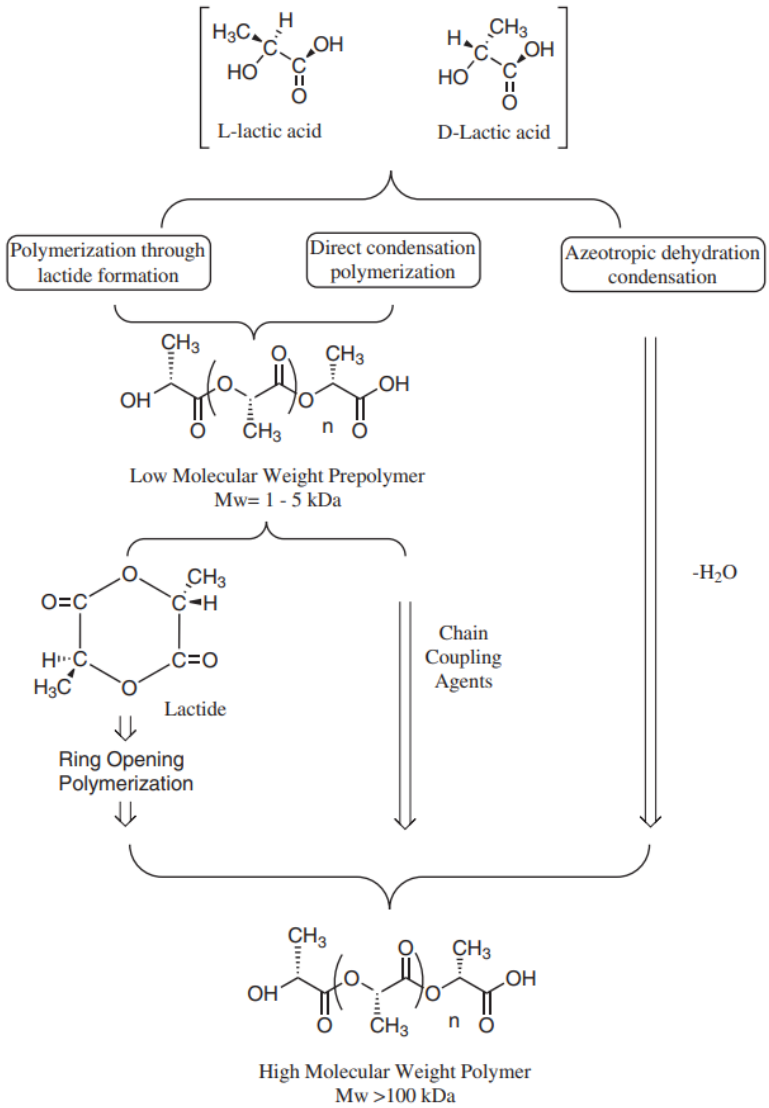

Figure 7 Production Process of PLA [29]

As we previously established, polylactide comes in a variety of shapes because lactic acid is chiral. The end result of L-lactide polymerization is poly-L-lactide (PLLA). Advances in technology have expanded the production of the D-enantiomer. Normally amorphous poly-DL-lactide (PDLLA) is produced by polymerization of a racemic mixture of L-lactide and D-lactide [36][39]. Crystallinity has been observed in heterotactic PLA prepared using stereospecific catalysts. The degree of crystallinity and consequently many important properties are determined by the ratio of D to L enantiomers, but also to some extent by the type of catalyst used. It is also claimed that PLA-like polyhydroxyalkanoates can be produced directly. PLA polymers have moduli in the range of 2.7–16 GPa, glass transition temperatures of 60–65 °C, and melting temperatures of 130–180 °C [37]. Young's modulus is a fundamental property of any material. Different materials can have the same elastic modulus, but the elastic modulus remains the same unless the same product component is changed. Also called elastic modulus, it describes the stiffness of a material. In other words, it is easy to bend and stretch. Physics explains that Young's modulus is determined by the ratio of stress and strain. Stress is the ratio of force to cross-sectional area. Elongation is the ratio of the length of a material to the change in original length. Every material can withstand a certain amount of tension. When you apply enough force to exceed this stress point, the molecules or atoms of the material will begin to deform. This causes permanent changes in its chemical structure, shape, usability, etc. For example, when you stretch a tire, it can return to its original state without being deformed. However, if you use too much force, the tire will break and cannot be restored [35]. The Young's Modulus is very important to engineers and scientists because this constant can tell them when a structural implant will deform. This will allow them to know how to mechanically design a part for use in a body. When Young modulus graphed, the resulting plot will look like in the Figure 8.

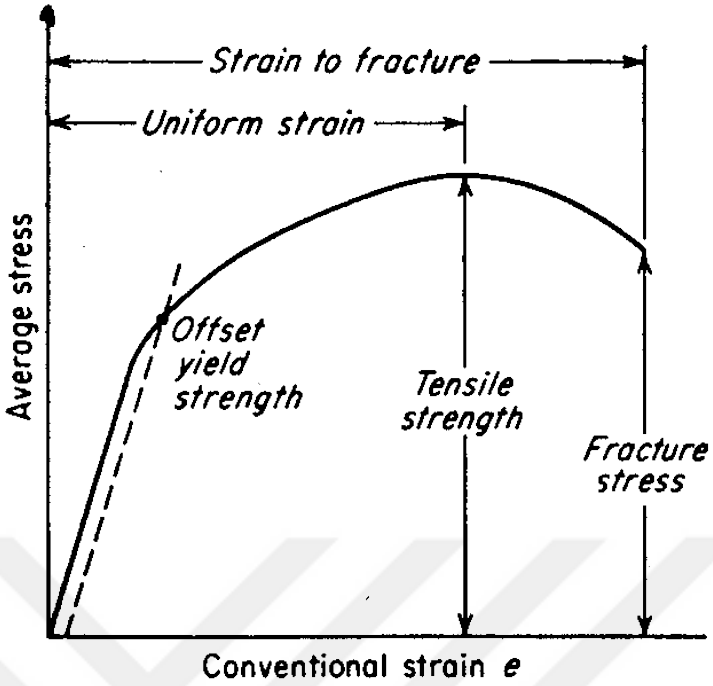

Figure 8 Young Modulus [68]

PLA is able to tolerate temperatures of 110 °C. PLA's fundamental mechanical characteristics fall in between those of PET and polystyrene Polymers and PDLA can be physically combined to increase the melting temperature of PLLA to 40-50 degrees Celsius and the heat distortion temperature to 190 degrees Celsius (poly-D-lactide). PDLA and PLLA together form a highly ordered stereocomplex with higher crystallinity. Temperature stability is highest when using a 1:1 mixture, but significant improvement is seen when the PDLA concentration is lowered to 3-10%. In the latter case, PDLA acts as a nucleating agent that speeds up the crystallization process. PDLA degrades more slowly than PLA because it has a stronger crystallinity. PLA has a higher flexural modulus than polystyrene and is well-suited for heat sealing [39].

A variety of organic solvents can dissolve PLA. Because it is accessible and minimal danger, ethyl acetate is commonly used. It is helpful for removing PLA supports from 3D printers and for cleaning the extruder heads. Propylene carbonate, which is safer than ethyl acetate but harder to find commercially, is another safe solvent. Pyridine can also be used, but is less safe than ethyl acetate and has a stronger fishy odor. Tetrahydrofuran, dioxane, and heated benzene are also soluble in PLA.

2.3. 3D Printing Technology

3D printer technology, which has come a long way since 1940, has gained wide acceptance in the field of manufacturing. It has become popular in short and medium-term production thanks to its price performance, accessibility, and ease of use. It has been said that 3D printing is a fantastic technique for combining or depositing materials to build objects. Once the final shape of the object is achieved, this process is repeated layer by layer. It allows us to transform structures directly from 3D design drawings into innovative and versatile products. Sharp changes can be made to the materials, down to the smallest detail, without spending a long time in a certain molding process.

The closest idea to 3D printing was described in the 1940s by Murray Leinster in his book Things Pass. In Murray's words, 'This moving arm transforms the area scanned by photocells into drawings in the air' [44]. Similar terminology is used in Raymond Jones' 1950 short tale "Tools of the Trade," which appeared in the Astounding Science Fiction magazine. In 1971 Johannes F. Gottwald developed the Liquid Metal Recorder. It is a continuous inkjet metal material machine that produces removable metalwork on reusable surfaces that can be used immediately or remelted and stored for printing [46][47]. This appears to be the first patent to mention rapid prototyping and regulated on-demand patterning in relation to 3D printing. The term "printing" has no specific meaning according to the patent and may instead refer to the use of ink to create or create another symbol, letter or pattern. The term "ink" as used covers any flowable substance or composition suitable for application to a surface to form a symbol, letter, or information pattern by marking, as well as dye- or pigment-containing materials intended to be Hot melt ink is the preferred type of ink. At this time, it is unclear what types of commercially available ink compositions can meet the requirements of the present invention. However, using the conductive metal alloy as ink, satisfactory printing in accordance with the invention has been accomplished. In addition, Johannes mentioned that in order for a production of this scale to be continuous, it should have an increase in size and an intelligence model of its own. Without a doubt, this means high costs in the conditions of that period. The first research that most closely corresponds to the noun meaning of 3D printers and is accepted as the beginning of 3D printers was done by Hideo Kodama. When using photocurable thermoset polymers, Kodama developed two additive processes for creating three-dimensional plastic models. The UV exposure area is controlled by a mask pattern or a scanning fiber transmitter [48]. In 1981, he tried unsuccessfully to patent his plotter with XYZ axes[49].

On July 2, 1984, American businessman Bill Masters applied for a patent for a computer-assisted manufacturing system and process. This application is the first of his three master patents that laid the groundwork for his modern 3D printing technology, and as his first ever 3D printing patent he filed with the USPTO. Most of his 3D printers on the market today, in 1988 he built S.H.I.E.L.D. Scott Crump was commercialized by his company Stratasys, which released the first FDM machine in 1992 [53]. Emanuel Sachs invented his powder bed technology in 1993 at MIT using conventional and custom inkjet his printheads commercialized by Soligen Technologies, Extrude Hone Corporation, and Z Corporation. This process gave rise to the term "3D printing". To develop a self-replicating rapid prototyping machine, Dr. Adrian Bowyer founded his RepRap open-source project in 2005. They have developed a 3D printer that can print most parts and in 2008 he developed the RepRap 1.0 "Darwin". I made an exact duplicate of the part and achieved the first self-replication. The open source components of the project were developed on his RepRap forum. At this forum, people from all over the world created original concepts and designs for his 3D printer. Posts on these forums are contributing significantly to the latest innovations in 3D printers. The Fused Deposition Modeling (FDM) printing process patent expired in 2009 [54]. This allows new companies to start manufacturing commercial FDM 3D printers. Many of them were generated by the RepRap community. FDM or FFF 3D printers can now print with a wider variety of plastics thanks to the plastic-to-close loop method developed by Filabot in 2012. When the price of printers started dropping, people interested in this technology were free to create whatever they wanted. Commercial printers are still expensive, over $2,000 as of 2014. However, certain DIY printing kits may be purchased for about $400, giving amateur printers access to printing techniques not used in production or industry. Fused deposition modeling, or FDM, is a material extrusion technology that accounts for 46% of all 3D printing processes as of 2018 [55][56].

Today, 3D models are made using computer-aided design (CAD) [58]. Compared to other production techniques, this one produces less errors. because mistakes in 3D models can be found before printing and fixed digitally. The final appearance of the thing can be predicted before it is created by utilizing an appropriate scanner or by creating a digital sketch. The intended object should initially be printed in tiny and standard resolution to increase the accuracy rate. Its layered structure has the potential to produce the stair step effect, much like all other additive manufacturing techniques. The orientation of a part surface throughout the building process has a significant impact on the outcomes. For overhanging elements, several

printing processes demand the building of internal supports. After the print is finished, these supports must be mechanically eliminated or dissolved [57]. Due to the simplicity of handling and producing polymeric materials, 3D printing has traditionally centered on printing with polymers. However, the process has quickly advanced to enable the printing of metals, ceramics, and other materials in addition to different polymers and making 3D printing a flexible production alternative.

However, there are a number of drawbacks to using 3D printing technology. For instance, the use of 3D printing technology would decrease the need for manufacturing labor, which will immediately have a significant impact on the economies of nations that heavily rely on low-skill occupations. Additionally, users of 3D printing technology can manufacture a wide variety of objects, including knives, firearms, and other hazardous goods. In summary, it will show beneficial effects when used correctly, but there are still aspects that need to be discovered and developed. This thesis combines PLA material, which we use everywhere in our lives, with 3D printer technology and explains its mechanical limits.

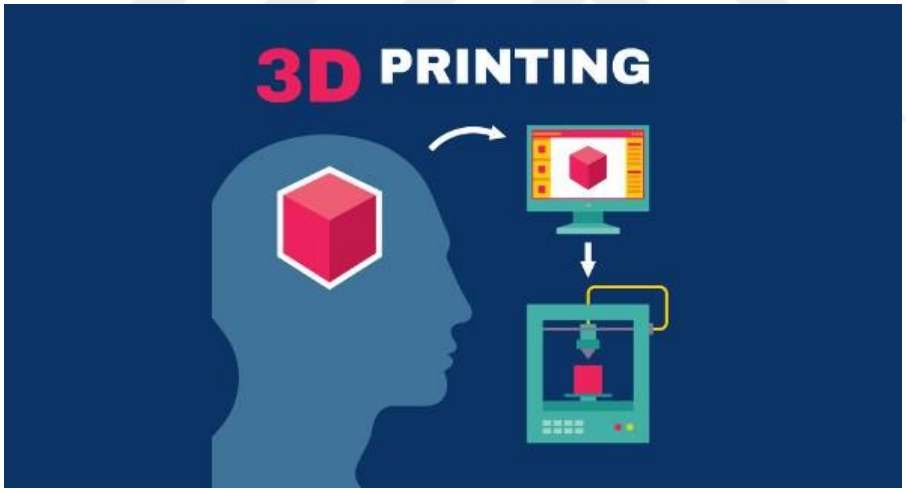

Figure 9 3D Printing [63]

2.4. PLA Filament

PLA filament has ease of transportation and use. PLA is more suitable for users who are new to 3D printers. One of the most common problems during printing for a 3D printer is bending/lifting. This is because during printing, due to the cooling of the material in the first layers, the material shrinks and separates from the bed and affects the other layers. Another problem is the formation of cracks in the upper layers of the printed part. In PLA materials, there is no problem with lifting in the first layers and cracking in the later layers. Also, you can separate the printed part from the bed more easily with PLA. It has a bright appearance and usually does not smell bad during printing. It is very important that it can operate at a low printing temperature compared to its peers and that it almost does not need bed temperature. The PLA filament may not always be mechanically adequate due to its fragility and low melting point. However, we mentioned that this mechanical range can change with different production methods. On top of that, it is made suitable for the purpose by adding different metals to its content. Currently, the price of PLA filament may change according to the colors and qualities you choose. The cost may increase due to hybrid filaments like conductors and wood. The cost of a desktop filament is typically between 20 and 70 euros per kilogram.

The only drawback is that the PLA filament has a higher viscosity which can clog the print head (nozzle) if you are not careful. There are many articles about this clogged nozzle causing health problems. In addition, all 3D printed products have cracks and small holes in them. Although it has not been fully proven yet, it is thought that bacteria accumulating in these cavities cause health problems. The fact that they cannot be washed in the dishwasher strongly supports this idea.

Figure 10 Clogged Nozzle [64]

Table 2 Properties of PLA Filament [62]

Property:	**PLA**
3D Printing Requirements:	
Printing temperature	180 - 220 °C
Print bed temperature	20 - 60 °C (optional)
Enclosure	Optional
Print fan	Recommended
3D Printing Difficulties:	
Nozzle clogging	Occasionally, due to thermal expansion & viscosity
Warping	Rarely
Moisture absorption in storage	Yes
Fumes during printing	Little to none
Material properties:	
Strength	Good
Flexibility	Brittle
Impact resistance	No
Density	1.2 - 1.4 $g \cdot cm^{-3}$

The table 2 and 3 shows some of the important specialties of PLA filament. Such as mechanical-thermal properties, and printing requirements. The values shown in the image depend on the brand of PLA filament and the 3D printer used. In addition, environmental conditions are also effective.

Table 3 Thermal Properties [62]

Property:	PLA
Glass transition temperature	57 °C
Melting point	150 - 160 °C

2.5 Comparison of 3D Printing and Other Production Methods

When it comes to mass production, traditional manufacturing techniques are recognized to be effective. These, however, are not the best option when specific prototypes, including pilot parts, spare parts, low-volume production series, tools, or jigs are required because of their high setup costs. With 3D printing technology, there are no major set-up costs and parts can be produced directly from the digital model. No molds are required with 3D printing, which has a great advantage in terms of cost control. Making molds, ramping up plants, and acquiring material blocks are necessary in order to start production using traditional manufacturing techniques. The process is generally lengthy, and it typically takes 15 to 60 days to receive the initial parts. The costs indicated above are eliminated when using 3D printing, and the initial sections can be finished the very next day. Products may be manufactured efficiently and delivered fast, which speeds up market entry. Additionally, it enables rapid responses in production and on-the-fly modification of parts.

For instance, to pay the general costs of tooling, assembly work, and production, injection molding requires large-scale production. To keep the unit costs of the manufactured parts reasonable, the production series must be vast because even a simple mold might cost thousands of dollars. This causes expenditures in inventory management and raises the risk for the user or buyer when it comes to low-volume parts. One benefit of 3D printing is that the complexity of the manufactured parts doesn't raise the cost of production.

Subtractive manufacturing techniques include removing material from the material block until the component is complete. There are two difficulties. The material loss in this kind of manufacturing is often considerable, reaching up to 70–80% of the initial block. Second, there aren't many material building blocks available, particularly for high-performance polymers and

polymer composites. These limitations do not apply to 3D printing. The manufactured pieces have almost no material loss, and their geometries can be quite complex and functional.

Contrary to traditional manufacturing techniques, 3D printing enables the direct production of items where they are required. As a result, physical inventory is not as necessary, and inventory management is improved. Whereas parts made using traditional techniques must be manufactured/purchased in bulk, 3D printing allows the production of single parts as needed. 3D printing has significantly lower manufacturing costs for individual components, prototypes, and production aids. This enables risk-taking design experiments and excellent outside-the-box thinking, which are more likely to result in remarkable inventions. In order to ensure the best possible client experience, an unlimited number of adjustments can also be made to existing items depending on consumer feedback. When compared to iterative rounds of product development using traditional manufacturing techniques, 3D printing can be up to 90% cheaper and faster.

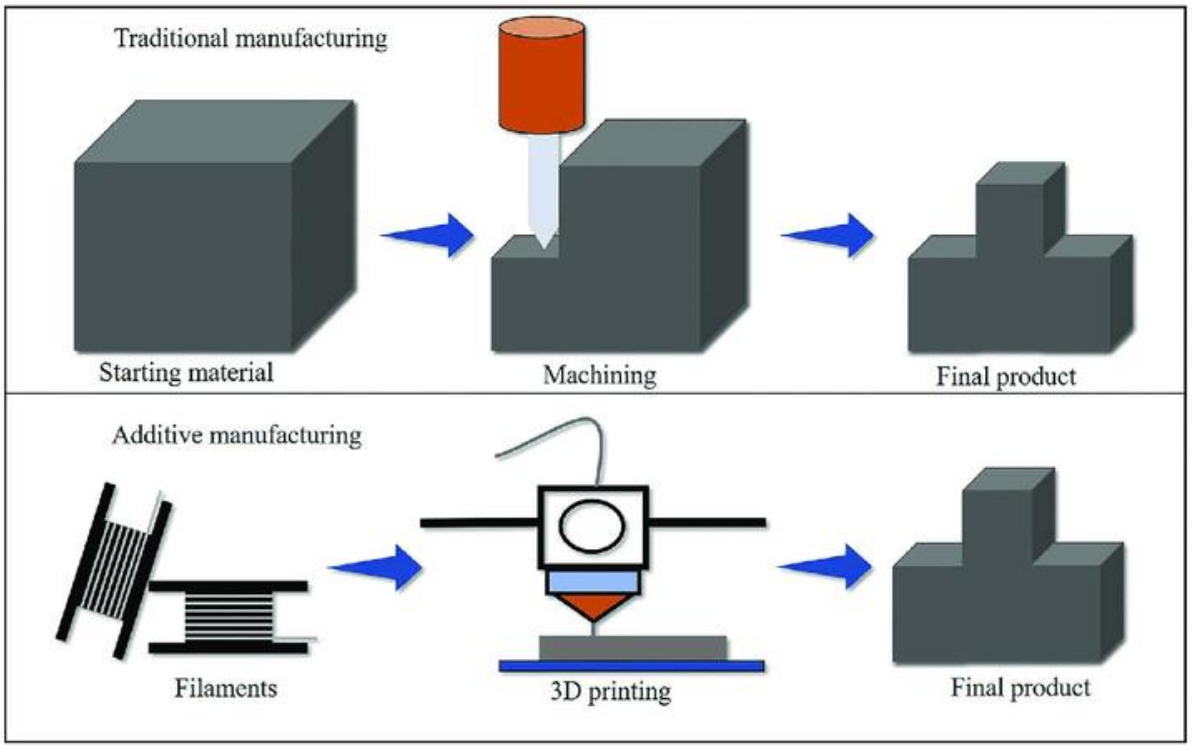

Figure 11 Traditional Manufacturing vs. Additive Manufacturing [61]

3. MATERIALS AND METHODS

3.1. Printer and Testing Machine Selection

Anycubic's i3 Mega is regarded as being among the best low-budget 3D printers for amateur users currently available. The success of the Mega series is due to sturdy build quality and impressive printing results, all for an attractively low price point. Anycubic is a stunning, sturdy printer that will fit anywhere in the house because of its simple, desktop design. It boasts a sturdy, well-constructed bent sheet metal chassis composed of high-quality parts. The loss of print quality on large portions is prevented by this sturdy and strong frame. Its structure is pre-assembled and may be put to use right out of the box with only a few minor changes. Even the absolute beginner will find it simple thanks to a rather comprehensive instruction booklet.

The package also includes a tool kit, a filament coil and its container, an SD card, and a USB drive with print-ready test files. Anycubic has introduced a touch screen display with a simple, intuitive user interface to replace the standard roulette screen. It has advanced features typically found in expensive printers. These include a filament detector, that stops printing until the filament is changed, or the auto-calibration function, which will automatically level the two Z-axis spindles to have them perfectly balanced. The Ultrabase Anycubic base together with the heat bed facilitates the bonding and subsequent debonding of components ABS and other challenging materials can be printed when the temperature of the heat bed exceeds 110 degrees. The print base reaches the proper temperature in a short period of time, making it a fast and adaptable printer that works with most materials. The hot end of Anycubic i3 Mega has a maximum temperature limit of 260 °C. This is more than adequate for printing with all of the common plastics, such as PLA, ABS, and PETG, but not hot enough for high-performance filaments, such as nylon. The typical 0.4 mm brass nozzle offers good performance and compatibility with a variety of filaments. However, it is recommended to avoid using it for printing with carbon fiber or other abrasive materials as they can destroy the nozzle and rub through the brass. The workspace of the Anycubic i3 Mega is not closed, which is advantageous for materials that can cause excessive smoke and odor during production. On the contrary, fast blowing wind or accidentally spilled liquid on the bed surface may cause the entire production to be reset. In all circumstances, care should always be taken when using simple printers. For visualization check figure 12 down below.

Figure 12 Anycubic I3 Mega [60]

For the testing machine; Shimadzu, one of the world's leading machine manufacturers for analytical instrumentation and testing equipment. The AGX series, which is the result of more than 100 years of experience, includes many new technologies in today's conditions. It offers a measuring range of 0-600 kilonewtons, as well as improved operability and the highest measuring capacities. Besides, it has software that supports high accuracy, adaptive test heads, multi-processor, a high degree of security, and data processing. This device is used in the field of transportation, especially in the aircraft industry, and in the composite material industry. PLA has a low strength compared to other materials used in the industry [76]. The wide working range of Shimadzu and the high accuracy rate in this range are important for the results of the study.

Figure 13 Shimadzu AGX [81]

3.2. Zigzag Filled Samples

Based on the Shimadzu tensile test mold's dimensions, Solidworks was used to create the part's drawing. The PLA samples were 3D printed using a normal 1.75 mm PLA filament on an Anycubic i3 Mega 3D printer. The nozzle and table were 200 and 60 degrees Celsius, respectively. An intermediate pace for 3D printing, 50 mm/s, was chosen as the printing speed. Figure 14 depicts the sample's measurements. The fracture sample thickness was 10 mm. The Cura 4.4.1 program was used to compile the 3D printing g-codes. The most common style of filling in actual practice, zigzag, was chosen as the first filling pattern. In addition to one variant with a filling ratio of 40% and a 0.3 mm nozzle to test the effect of nozzle diameter, five distinct types of 3D-printed PLA samples with filling ratios of 20, 40, 60, 80, and 100% were employed in the studies. Figures 15 and 16 display the cross-sections of these six fracture samples with varying filling ratios. To test the 40% fills with a 0.2 mm nozzle variation at angles of 0, 15, 30, 45, 60, 75, and 90°, a total of 21 samples were needed. Three samples were used to test each angle. The other five variants, which were to be assessed using three samples each at angles of 0, 45, and 90°, each required the creation of nine samples. The tests' main goal was to ascertain how the filling ratio affected the samples' fracture behavior in mode I, mode II, and mixed modes. To analyze the alteration in the mixed-mode fracture behavior with 15° increments and the impact of a bigger nozzle diameter of 0.3 mm, which is not a regular printing dimension but is utilized for draft printing, a version with 40% filling was chosen as the reference. Figure 17 demonstrates how a fragmented sample can be produced using a 3D printer.

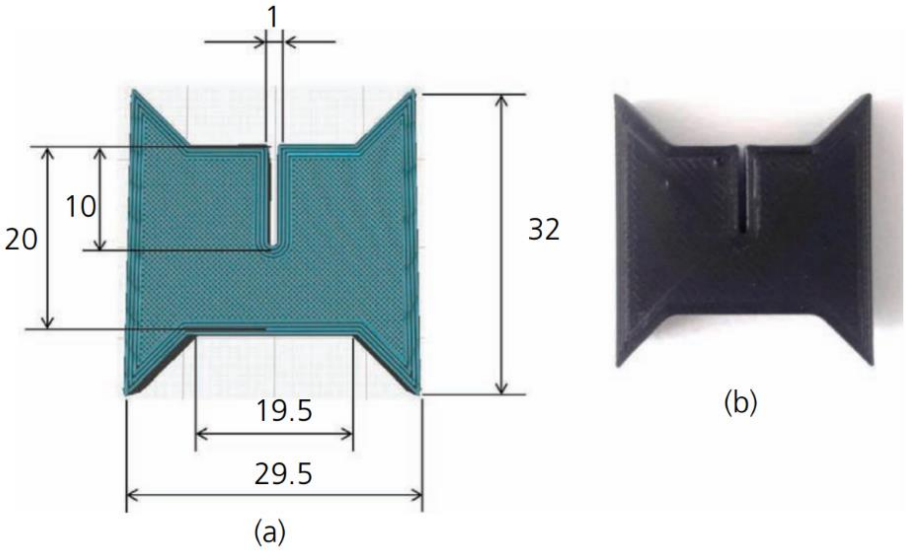

Figure 14 (a) Drawing (mm) (b) Basic shape of sample [67]

Figure 15 20% 40% 60% 80% and 100% filling rates respectively (0.2 nozzle diameter-zigzag) [67]

Figure 16 %40 filling rate (0.3 nozzle diameter) [67]

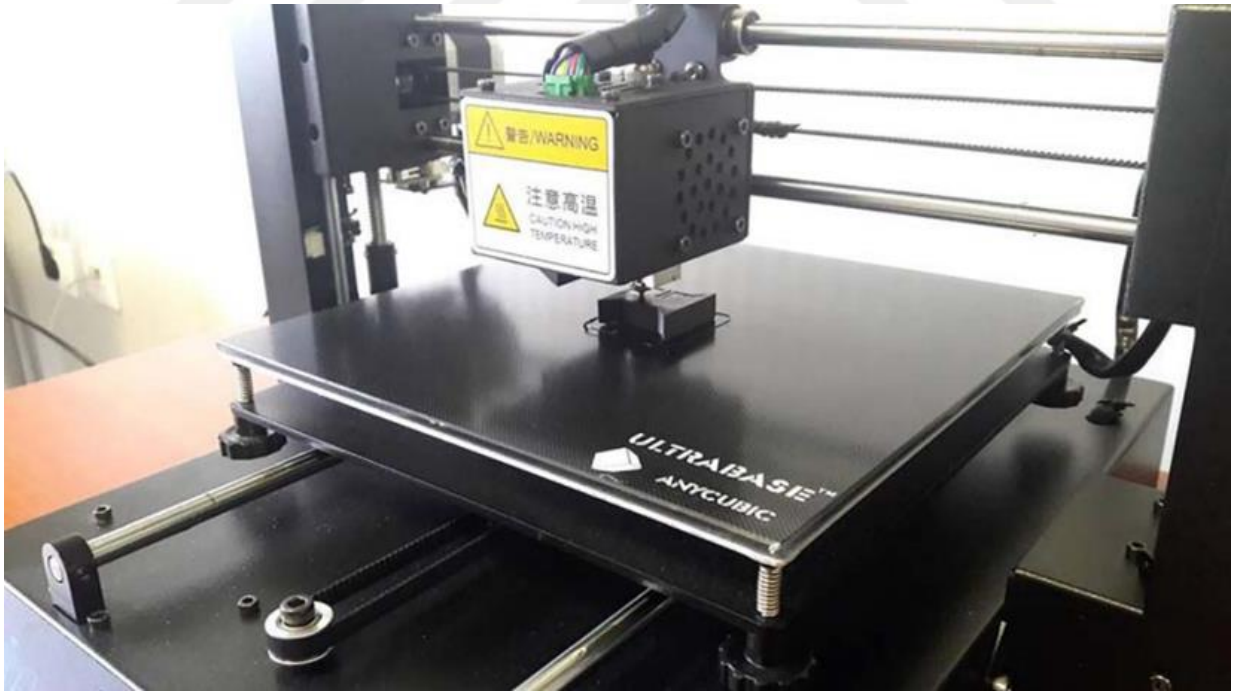

Figure 17 Production phase using Anycubic [67]

Table 4 summarizes the elastic constants of the fixtures and samples used in the finite element analysis. 3D-printed PLA dog bone samples with different zigzag filling ratios were prepared and evaluated according to the ASTM D 638-03 standard to determine their mechanical properties. The law of mixture was used to determine how the fill factor affects the modulus of elasticity. Poisson's ratio was extracted from the literature and found to have little effect on finite element analysis. The results show that the stress-strain curves of 3D-printed PLA with different zigzag filling fractions are linear, indicating that linear elastic behavior can be assumed for this material.

Table 4 Elasticity Modulus and Poisson Ratio, Comparison with Steel [67]

Materials	PLA 20 %	PLA 40 %	PLA 60 %	PLA 80 %	PLA 100 %	Steel EN 1.4016
Modulus of elasticity (GPa)	0.7	1.4	2.1	2.8	3.5	200
Poisson's ratio (-)	0.36	0.36	0.36	0.36	0.36	0.3

3.3. Gyroid Filled Samples

In order to reveal the behavior patterns of material structures, which is the main goal of this article, we add samples filled in the form of Gyroids. At the point where all variables remain constant, only Zigzag filled samples as well as Gyroid ones will be subjected to the same test. The internal cross-sectional structure of the PLA samples filled with gyroids is shown in figure 18. Vertical and horizontal sinusoidal waves are sequentially combined to form the gyroid type filling. It is feasible to strengthen the toughness of rather brittle polymers like PLA by making use of the wavy internal structure of the gyroid filling. The filling ratios in the samples were 20%, 40%, 60%, 80%, and 100%; since a gyroid filling could not be produced for 100% of the filling, zigzag filling was used instead. The results demonstrate that the stress-strain behavior of 3D printed PLA with gyroid type filling was linear in accordance with ASTM D638-03. The finite element analysis therefore makes the assumption that it is linearly elastic. Table 3 is also acceptable for the gyroid form. To ascertain the geometric properties of the samples, which are then used to ascertain the fracture toughness, finite element analysis is required. You can see the inside of the gyroid filled samples in figure 18. The wavy structure that mentioned is more evident in samples with low filling ratio, such as 20%. As the filling rate increases, this salience decreases as the wave frequency increases.

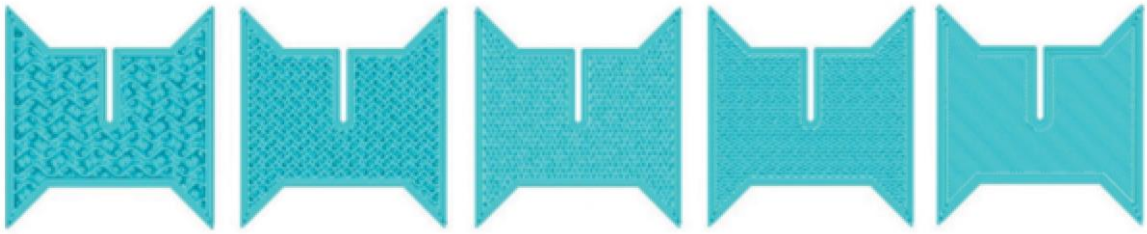

Figure 18 20% 40% 60% 80% and 100% filling rates respectively (0.2 nozzle diameter-gyroid) [65]

3.4 Testing Methods and Finite-Element Model

In cracks, there are three distinct fundamental loading modes. Mode I, or the opening mode, is produced by typical stresses. Shear stresses lead to Mode II, often known as the shearing mode. An out-of-plane shear leads to Mode III, also referred to as the ripping mode. The primary difficulty in forecasting material failure is determining the fracture toughness for the three modes of loading (I, II, and III), particularly under mixed-mode loading conditions. A modified version of the Arcan specimen was developed for the mixed-mode fracture testing of 3D-printed PLA with different filling ratios. This specimen enables testing of pure mode I, pure mode II, and almost any combination of mode I and mode II. With the same test specimen design, loading angles of 0°–90° can be achieved in 15°steps (Figure 19). The fixture allows two different sizes of test specimens to be tested for fracture. For this study, a small size was chosen to save both resources and time (Figure 14). Figure 20 shows the load fixture consisting of the specimen and her two grips. The sample is attached to the holder and the holder's handles are separated by her two handle holes on either side of the radial line for sample loading. 4000 series steel was used in its construction to ensure that the device had sufficient strength and dimensional stability for destructive testing. By varying the load angle, (a = 0°, 15°, 30°, 45°, 60°, 75°, and 90°), all mixed modes from pure mode I to pure mode II can be set up and tested. increase. While maintaining a constant displacement rate of 0.5 mm/min, a rupture test was performed to measure the rupture load and displacement. Each test was performed using a Shimadzu testing machine. Maximum load and displacement were calculated using the load-displacement curve generated by the tester. Linear elasticity describes the normal load displacement relationship for mixed-mode failure in 3D-printed PLA samples.

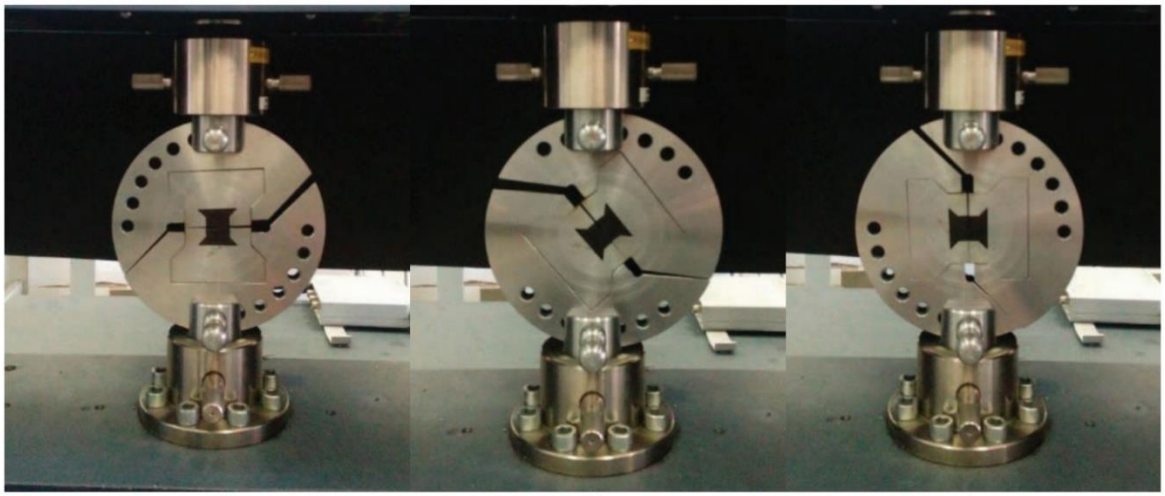

d

Figure 19 Testing Modes a) Tensile b) Mixed c) Shear [67]

(a)

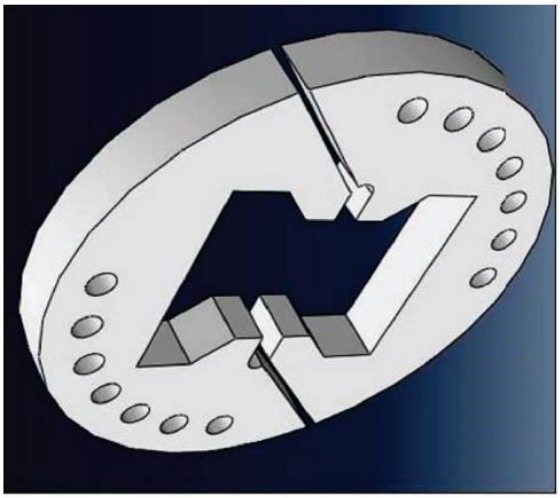

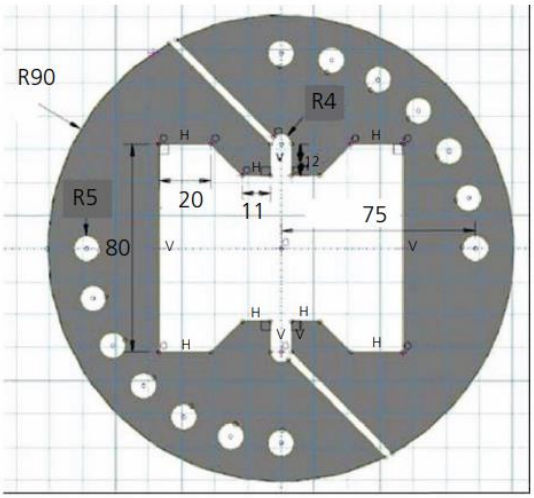

(b)

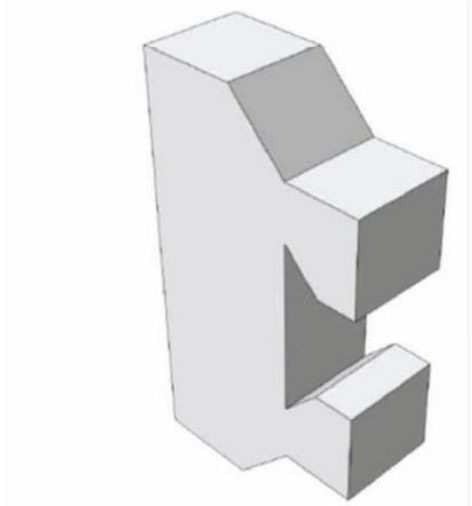

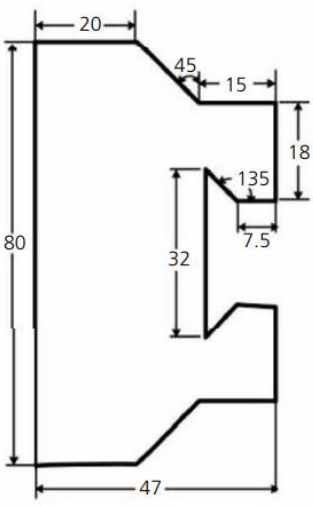

Figure 20 (a) Dimensions of outer fixture (mm) (b) Dimensions of inner fixture[67]

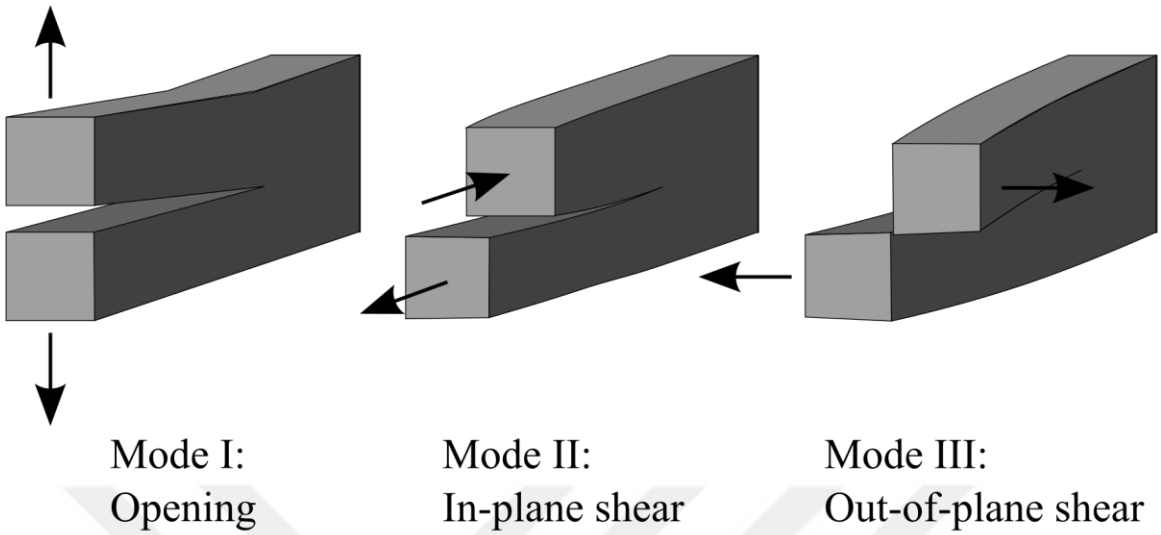

Figure 21 Fracture Modes [77]

We will look at the fracture characteristics of PLA, a material used in 3D printing, to better understand the mechanics of fracture. When evaluating the resistance of fractures, the J-integral and stress intensity parameters are typically used. It was decided to use the j-integral formulation for the finite element analysis. The J-integral can be used to calculate a material's strain energy release rate, also known as work per unit fracture surface area. The strain energy of a crack in a body under a constant load is equal to the oscillation rate. Only materials that behave linear elastically in quasi-static conditions often display this [80]. When materials display small-scale yielding around the fracture tip under particular conditions like monotonic loading in mode III, J can be used to calculate the energy release rate. There is no analytical solution for the stress intensity correction factors of the current sample geometry. Finite element analysis was utilized to ascertain this. Figure 22 displays a mesh model of the entire loading device and sample created with the Abaqus finite element code. As a result, the mesh was adjusted to be more precise at the fracture tip, and an eight-node collapsed rectangle element was used to model the complete sample with the first crack (CPE8R). The triangular and six-node shape of the cracked-end elements should be noted (CPE6M). Around the crack point, the crack is divided into five outlines. The element form gradually transforms as one moves away from the crack point into rectangles with a nearly 2:1 aspect ratio. The computed stress intensity factors were seen to remain unchanged as the number of elements grew. An interaction J-integral technique was used to analyze the stress intensity factor values. Utilizing the

$1/r^{1/2}$ stress field singularity, a linear elastic finite element analysis was carried out under a planar strain condition. It is broken up into sections that can be used to simulate a two-dimensional example. Due to the linear elastic finite element analysis, which transported the mid-nodes of both sides to the fracture point, the strains and stresses were square root singular. This approach was applied to the initial ring of components surrounding the fracture tip.

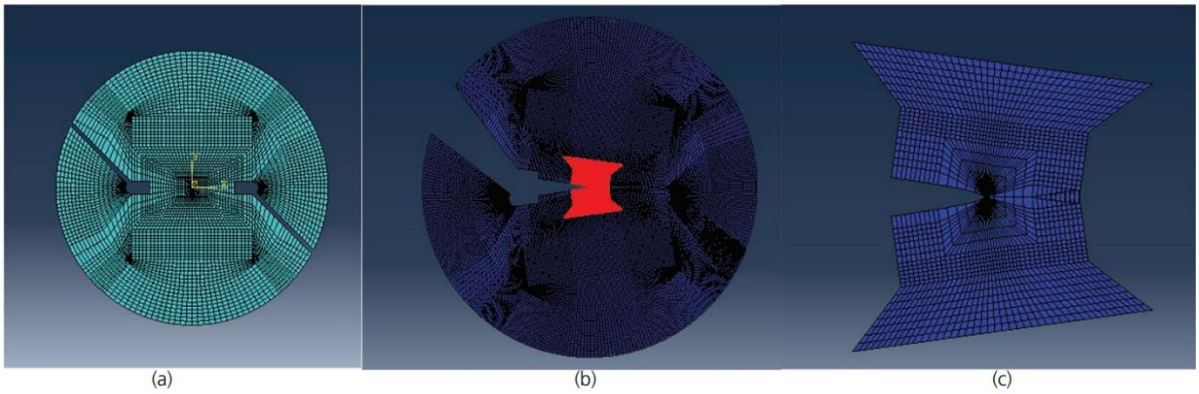

Figure 22 Three different views of Abaqus Finite Element Analysis [65]

4. RESULTS AND DISCUSSIONS

4.1. Results For Zigzag Filled Samples

Formulas 1 and 2 below describe the stress intensity factors K_I and K_{II}. Geometrical factor or non-dimensional stress intensity factors $f_I = (a / w)$ and $f_{II} = (a / \omega)$ for both samples and different loading angles were determined [72][76].

$$K_{\mathrm{I}} = \frac{P_{\mathrm{C}}(\pi a)^{1/2}}{wt} f_{\mathrm{I}}(a/w)$$

Eq1.

$$K_{\mathrm{II}} = \frac{P_{\mathrm{C}}(\pi a)^{1/2}}{wt} f_{\mathrm{II}}(a/w)$$

Eq2.

The geometrical components for various filling ratios under various loading orientations are compared and summarized in Table 5. As can be observed, for all filling ratios, the $f_I = (a / w)$ geometrical factor reduces, and the $f_{II} = (a / \omega)$ geometrical factor rises as the shear loading contribution climbs. This table shows that Mode I failure is dominant for loading angles below 60° and Mode II failure is dominant for loading angles between 60° and 90°. The geometrical factors $f_I = (a / w)$ and $f_{II} = (a / \omega)$ for different filling ratios were confirmed by finite-element analysis to be nearly consistent as the stiffness of the filling ratios varied.

Table 5 Angles and Geometrical Factor Values [65]

Loading angle	0°	15°	30°	45°	60°	75°	90°
f_I (a/w)	3.76	3.64	3.26	2.66	1.88	0.98	0
f_{II} (a/w)	0	0.3	0.58	0.82	1.01	1.13	1.17

The current values and the stress intensity factor equation in Table 5 are the same for both filling types. The critical fracture load Pc (N) in the equation will vary depending on the filling type and angles. This will allow us to get different results, in this way, the filling type comparison will be made more logical.

Fracture tests were performed using a Shimadzu tensile tester while maintaining a displacement rate of 0.5 mm/min. This procedure was then repeated three times for each load angle and the average failure load was recorded. Mode I, Mode II, 45°, and five other mixed mode loading situations were applied for each of the filling fractions, as shown in Table 6. The table shows that the critical failure load increases with shear load, with increasing contributions at all filling degrees. At a constant fill factor, as the nozzle diameter changes, the Mode I failure load increases relatively, while the Mode II failure load remains essentially constant. Comparison of 40% PLA-0.2 and 40% PLA-0.3.

Table 6 P_c (N) values for zigzag filled samples and angles [67]

Filling ratio	0°	15°	30°	45°	60°	75°	90°
20% PLA–0.2	1059.3	—	—	1059.5	—	—	1099.5
40% PLA–0.2	1216.1	1250.0	1300.6	1382.6	1442.8	1564.6	1579.3
40% PLA–0.3	1231.6	—	—	1442.9	—	—	1580.9
60% PLA–0.2	1479.6	—	—	1573.5	—	—	1702.0
80% PLA–0.2	1794.8	—	—	1909.4	—	—	2444.5
100% PLA–0.2	2180.0	—	—	2340.5	—	—	2714.5

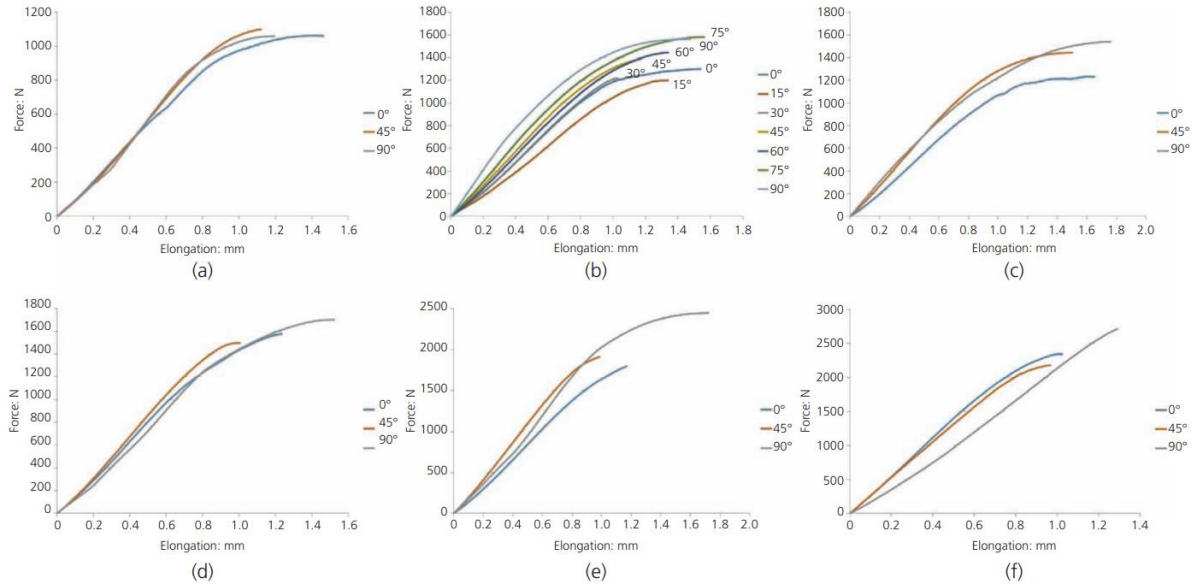

Figure 23 Force-Elongation Graph: A to F respectively filling ratios with 0.2 diameter except C (0.3). [67]

Figure 23 is a line plot of the force-elongation ratio of specimens subjected to tensile forces under different modes. Five different filling amounts (%) for the 0.2 mm sample; 20, 40, 60, 80, 100 and for the 0.3mm sample; only a 40% fill rate was used. 40% PLA-0.2 parts were also tested with an additional 15, 30, 60, and 75 degrees to see the cascade behavior of mixed mode loading. The first result that stands out directly; As the filling rates and degrees increase, the

maximum force values increase. This amount of increase is not very noticeable at only 20% PLA-0.2% and this change will not have a huge impact. See table 6 for a direct look at the numbers.

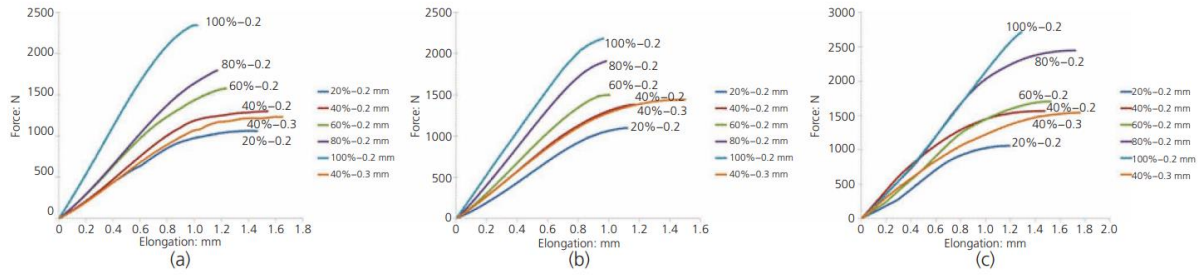

Figure 24 Force-Elongation Graph (a) Opening Mode; (b) mixed mode, 45°; (c) Shear Mode [67]

Figure 24 shows the same values arranged for mode I, mode II and mixed mode. The connection between maximum force and modes was mentioned. Increasing the nozzle diameter from 0.2 to 0.3 mm does not cause any change. Three different nozzle diameters are mainly used in 3D printers. Although the products produced with 0.1 mm have more details and high resolution, the production times are long. 0.3 mm ones can be produced more quickly and can be used in prototype tests. 0.2 mm has an optimum place in the middle of both.

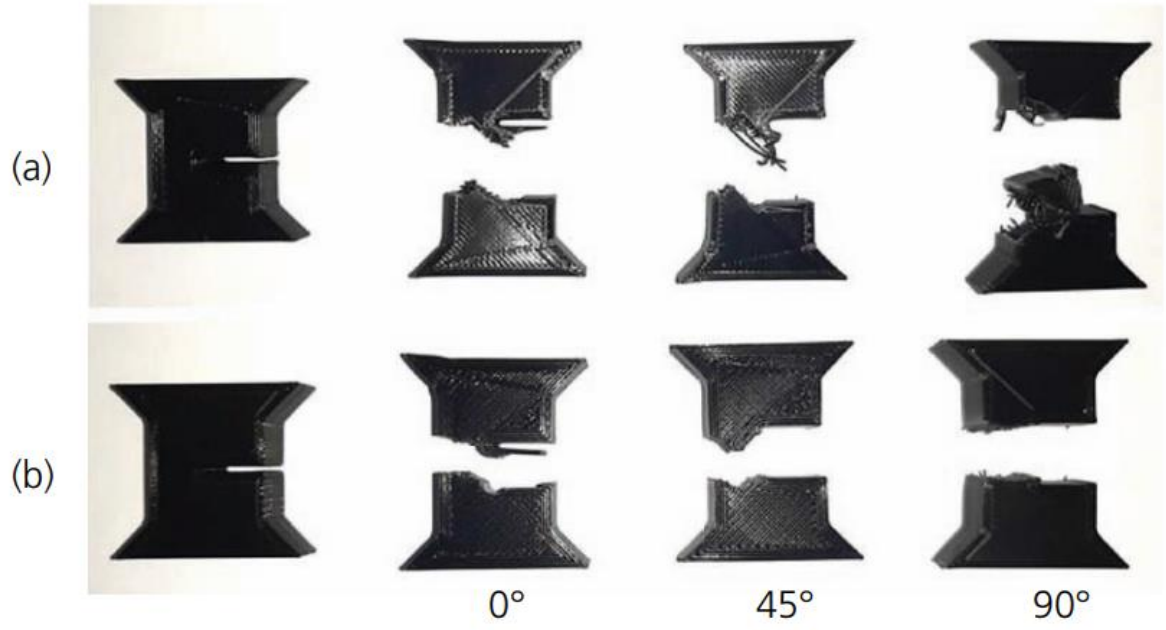

Figure 25 Before and after photos of zig-zag samples. In order of 0°,45° and 90° (a) 0.3 nozzle diameter %40 filling rate (b) 0.2 nozzle diameter %100 filling rate [67]

Figure 25 displays the fracture pictures of two samples, measuring 40.0 mm and 100.0 mm. The fracture behavior is brittle if the filling ratio is larger. The sample was broken up by splitting and stretching as the fill rate dropped.

Table 7 Kc (MPa $m^{1/2}$) values for zigzag filled samples and angles [67]

Filling ratio	Critical stress intensity factor	0°	15°	30°	45°	60°	75°	90°
20% PLA–0.2	K_{IC}: MPa $m^{1/2}$	3.53	—	—	2.50	—	—	0
	K_{IIC}: MPa $m^{1/2}$	0	—	—	0.77	—	—	1.14
40% PLA–0.2	K_{IC}: MPa $m^{1/2}$	4.05	4.03	3.76	3.26	2.40	1.36	0
	K_{IIC}: MPa $m^{1/2}$	0	0.34	0.67	1.01	1.29	1.57	1.63
40% PLA–0.3	K_{IC}: MPa $m^{1/2}$	4.10	—	—	3.40	—	—	0
	K_{IIC}: MPa $m^{1/2}$	0	—	—	1.05	—	—	1.64
60% PLA–0.2	K_{IC}: MPa $m^{1/2}$	4.93	—	—	3.71	—	—	0
	K_{IIC}: MPa $m^{1/2}$	0	—	—	1.14	—	—	1.76
80% PLA–0.2	K_{IC}: MPa $m^{1/2}$	5.98	—	—	4.50	—	—	0
	K_{IIC}: MPa $m^{1/2}$	0	—	—	1.39	—	—	2.53
100% PLA–0.2	K_{IC}: MPa $m^{1/2}$	7.26	—	—	5.52	—	—	0
	K_{IIC}: MPa $m^{1/2}$	0	—	—	1.70	—	—	2.81

The mean data of the analytically discovered critical stress intensity components under different loading situations are shown in Table 4. For all filling percentages examined, K_{Ic} falls as the angle increases from 0 to 90° whereas K_{IIC} rises. It is interesting to notice from Table 4 that for all loading angles, the fracture toughness rises along with the filling ratio. The average fracture toughness of pure tensile loading is designated as K_{Ic} in the average values of fracture toughness data in terms of stress intensity components.

4.2. Results For Gyroid Filled Samples

As far as geometrical factors f_I and f_{II} are same, stress intensity factors K_I and K_{II} will remain the same. Therefore, the values in Table 5 are equally valid.

Table 8 P_c (N) values for gyroid filled samples and angles [65]

Materials and loading angles	0° (N)	15° (N)	30° (N)	45° (N)	60° (N)	75° (N)	90° (N)
PLA 20 %	1055.6			1093.1			1027.9
PLA 40 %	1349.2	1288.5	1287.3	1192.5	1516.7	1405.8	1180.6
PLA 60 %	1669.7			1692.0			1835.1
PLA 80 %	1775.2			1809.1			2235.3
PLA 100 %	2513.1			2681.7			2767.9

Look Table 8 for critical fracture load values of gyroid-filled specimens under the same test conditions. When the values are examined, the critical fracture load of the gyroid-filled samples, which have 20% and 40% filling rates, does not increase gradually. The numbers varied a lot

depending on the angle at which the test was performed. The values at 15-30-60-75 degrees, which we make extra for the samples with 40% occupancy, vary fluctuating. It continued to decrease from 0 to 45, and after making a sudden rise of 60 degrees, it started to decrease again. From 60%, the numbers increase as the angle and fill rate increase. Figure 26 displays 60% gyroid-type filled PLA samples that have undergone mixed-mode, mode-I, and mode-II fracture testing. Vertical and horizontal sinusoid curves are sequentially arranged to provide the gyroid filling. Internal structures of this kind prevent overly aggressive splitting action around the fractured location. Every sample produces fracture lines that continue the original horizont1al crack [65].

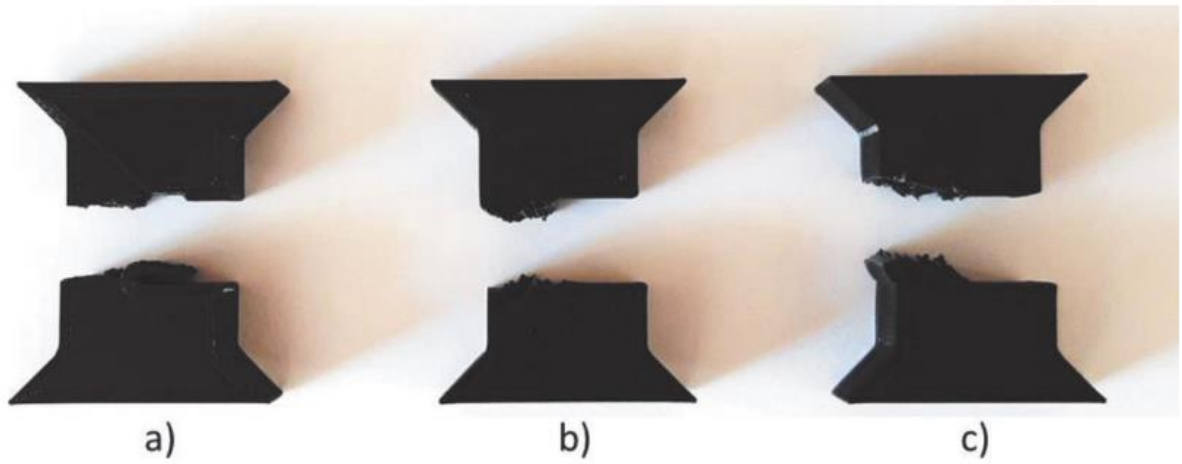

Figure 26 Fracture view of %60 gyroid filled sample a to c same modes [65]

Table 9 lists the experimentally determined values of fracture toughness at various loading angles. The results demonstrate that in tensile mode, the materials under consideration had significantly higher fracture toughness than in shear mode. Additionally, as the percentages of the filling ratios in the samples climbed, so did the tensile and shear fracture toughness. For all filling ratios, K_{Ic} declines, and K_{IIC} increases as rises from 0° to 90°. As a result, this is true for all loading angles: fracture toughness increases as filling rates do. In comparison to the typical zigzag-type filled PLA samples, the gyroid-filled PLA samples had a 40% increase in fracture toughness [67].

Table 9 Kc (Mpa $m^{1/2}$) values for zigzag filled samples and angles [65]

Materials and loading angles	0° (Mpa × $m^{1/2}$)	15° (Mpa × $m^{1/2}$)	30° (Mpa × $m^{1/2}$)	45° (Mpa × $m^{1/2}$)	60° (Mpa × $m^{1/2}$)	75° Mpa × $m^{1/2}$)	90° (Mpa × $m^{1/2}$)
PLA 20 % K_{IC}	3.51			2.57			0
PLA 20 % K_{IIC}	0			0.79			1.06
PLA 40 % K_{IC}	4.49	4.15	3.71	2.81	2.52	1.22	0
PLA 40 % K_{IIC}	0	0.34	0.66	0.87	1.36	1.41	1.22
PLA 60 % K_{IC}	5.56			3.98			0
PLA 60 % K_{IIC}	0			1.23			1.90
PLA 80 % K_{IC}	5.91			4.26			0
PLA 80 % K_{IIC}	0			1.31			2.31
PLA 100 % K_{IC}	8.36			6.31			0
PLA 100 % K_{IIC}	0			1.95			2.87

5. CONCLUSIONS

In this study, the fracture behavior of 3d printed PLA structures was analyzed. Tensile, shear, and mixed-mode tests were completed on samples using a Shimadzu machine, which samples produced by the Anycubic 3D printer. Abaqus finite element analysis was performed, and correction factors were obtained. As a result of the experiment, stress intensity factor, critical load, and elongation values were calculated. Visibly, these data are directly dependent on the fill level of the part and the type of filling. Although the degrees at which the test was carried out had a relative effect, the nozzle ratio did not cause a notable change. Pieces with different filling types at 40% occupancy gave different responses at 0-90 degrees. As the degree increased in the zigzag-filled samples, the critical fracture load increased proportionally, but the gyroid-filled sample reached the highest value at 60 degrees. There is a similar difference in the same degrees of stress intensity factor. Besides, the fracture and deformation patterns are different. Samples with a low fill rate are more prone to elongation. In general, samples with increased fill rates increase their durability, but when they come to the limit threshold, they break directly without stretching. However, it should be noted that there are many different factors, from the type of PLA to the fine-tuning of the test machine. Customizations to be made at any stage can directly affect the results. This is what makes PLA material special.

6. RECOMMENDATIONS

PLA material is very special with the features it offers and has. Increasing usage areas today should not be ignored and research should be continued in the future. It is most important for humanity that PLA is completely natural and does not harm nature. This study aimed to contribute to the use of PLA in the automotive and health sector. It can be combined with electrical applications and take place in vehicles, or it can be reduced to nano dimensions and its applicability to the human body can be investigated. Thanks to the carbon atoms it has, polylactic acid can be used in the most beneficial way in different areas in good hands. PLA has already been mixed with metal and other types of filaments for sale. Very common filaments such as ABS and PETG have versions containing PLA. Valid results were obtained even with only 2 different filling types and the same filament. 3D printing products today have dozens of different filling types and filaments, as well as increasing nozzle variations. For example, in the future, similar tests may be applied to samples produced with PLA copper material with a nozzle diameter of 0.4mm. The electrical conductivity of copper and the good aspects of PLA can contribute to the electricity sector.

REFERENCES

1. Biopolymers from Renewable Resources.; 1998. doi:10.1007/978-3-662-03680-8

2. Conn RE, Kolstad JJ, Borzelleca JF, et al. Safety assessment of polylactide (PLA) for use as a food-contact polymer. *Food and Chemical Toxicology*. 1995;33(4):273-283.

3. Jamshidi K, Hyon SH, Ikada Y. Thermal characterization of polylactides. *Polymer (Guildf)*. 1988;29(12):2229-2234.

4. Spinu M, Jackson C, Keating MY, Gardner KH. Material design in poly (lactic acid) systems: block copolymers, star homo-and copolymers, and stereocomplexes. *Journal of Macromolecular Science, Part A: Pure and Applied Chemistry*. 1996;33(10):1497-1530.

5. Lide DR. *CRC Handbook of Chemistry and Physics*. Vol 85. CRC press; 2004.

6. Garlotta D. A literature review of poly (lactic acid). *J Polym Environ*. 2001;9(2):63-84.

7. Painter PC, Coleman MM. Fundamentals of polymer science: an introductory text. Lancaster, Pa.: Technomic Pub. Co. Published online 1997.

8. Cação ADC. Development of new L-lactic acid copolymers: studies on the structure/properties relationship. Published online 2013.

9. Rasal RM, Janorkar A v, Hirt DE. Poly (lactic acid) modifications. *Prog Polym Sci*. 2010;35(3):338-356.

10. Scheele CW. *Chemical Observations and Experiments on Air and Fire*. J. Johnson; 1780.

11. Encyclopedia.com. “Karl Wilhelm Scheele .” Encyclopedia of World Biography. .

12. Daintith J. *Biographical Encyclopedia of Scientists, -2 Volume Set*. CRC Press; 1994.

13. Boeck G. Paul Walden (1863–1957): The man behind the Walden inversion, the Walden rule, the Ostwald-Walden-Bredig rule and Ionic liquids. *ChemTexts*. 2019;5(1):1-7.

14. Dorgan JR, Braun B, Wegner JR, Knauss DM. Poly (lactic acids): a brief review. Published online 2006.

15. Adams R. Wallace Hume Carothers. *National Academy of Sciences, Bio-graphical memoirs*. 1939;20:293-309.

16. Lunt J. Large-scale production, properties and commercial applications of polylactic acid polymers. *Polym Degrad Stab*. 1998;59(1):145-152. doi:https://doi.org/10.1016/S0141-3910(97)00148-1

17. Goodman M, D’Alagni M. Investigations of poly-S-lactic acid structure in solution. *J Polym Sci B*. 1967;5(6):515-521.

18. Kulkarni RK, Pani KC, Neuman C, Leonard F. Polylactic acid for surgical implants. *Archives of surgery*. 1966;93(5):839-843.

19. Middleton JC, Tipton AJ. MEDICAL PLASTICS AND BIOMATERIALS MAGAZINE. *March/April*. Published online 1998.

20. Gruber PR, Hall ES, Kolstad JJ, Iwen ML, Benson RD, Borchardt RL. US Patent, 5 258 488, 1993; b) PR Gruber. *JJ Kolstad, ES Hall, RS Eichen Conn, CM Ryan (Cargill Incorporated) US Patent*. 2000;6(143):863.

21. Drumright RE, Gruber PR, Henton DE. Polylactic acid technology. *Advanced materials*. 2000;12(23):1841-1846.

22. Vink ETH, Rábago KR, Glassner DA, et al. The sustainability of NatureWorks™ polylactide polymers and Ingeo™ polylactide fibers: an update of the future. *Macromol Biosci*. 2004;4(6):551-564.

23. Gupta B, Revagade N, Hilborn J. Poly (lactic acid) fiber: An overview. *Prog Polym Sci*. 2007;32(4):455-482.

24. Vink ETH, Rabago KR, Glassner DA, Gruber PR. Applications of life cycle assessment to NatureWorks™ polylactide (PLA) production. *Polym Degrad Stab*. 2003;80(3):403-419.

25. Linnemann B. M, S. Harwoko, T. Gries. *Chemical Fibers International*. 2003;53:426-433.

26. Castro-Aguirre E, Iniguez-Franco F, Samsudin H, Fang X, Auras R. Poly (lactic acid)—Mass production, processing, industrial applications, and end of life. *Adv Drug Deliv Rev*. 2016;107:333-366.

27. Södergård A, Stolt M, Inkinen S. INDUSTRIAL PRODUCTION OF HIGH-MOLECULAR-WEIGHT POLY (LACTIC ACID). *Poly (Lactic Acid) Synthesis, Structures, Properties, Processing, Applications, and End of Life*. Published online 2022:29-44.

28. Li G, Zhao M, Xu F, et al. Synthesis and biological application of polylactic acid. *Molecules*. 2020;25(21):5023.

29. Hartmann MH. High molecular weight polylactic acid polymers. In: *Biopolymers from Renewable Resources*. Springer; 1998:367-411.

30. Maleki H, Azimi B, Ismaeilimoghadam S, Danti S. Poly (lactic acid)-based electrospun fibrous structures for biomedical applications. *Applied Sciences*. 2022;12(6):3192.

31. Gritsch L, Conoscenti G, la Carrubba V, Nooeaid P, Boccaccini AR. Polylactide-based materials science strategies to improve tissue-material interface without the use of growth factors or other biological molecules. *Materials Science and Engineering: C*. 2019;94:1083-1101.

32. Young RJ, Lovell PA. *Introduction to Polymers*. CRC press; 2011.

33. J r me C, Lecomte P. Recent advances in the synthesis of aliphatic polyesters by ring-opening polymerization. *Adv Drug Deliv Rev*. 2008;60(9):1056-1076.

34. Kaur P. Literature Review: Ring Opening Polymerization of Polylactide. *J Emerg Technol Innov Res*. Published online 2018.

35. Moosbrugger C. Representation of stress-strain behavior. *Atlas of Stress Strain Curves, 2nd ed; ASM International: Materials Park, OH, USA*. Published online 2002.

36. Lunt J. Large-scale production, properties and commercial applications of polylactic acid polymers. *Polym Degrad Stab*. 1998;59(1-3):145-152.

37. Anders S. dergard, Mikael Stolt. Properties of lactic acid based polymers and their correlation with composition. *Prog Polym Sci*. 2002;27:1123-1163.

38. Fiore GL, Jing F, Young Jr VG, Cramer CJ, Hillmyer MA. High T g aliphatic polyesters by the polymerization of spirolactide derivatives. *Polym Chem*. 2010;1(6):870-877.

39. Park HS, Hong CK. Relationship between the stereocomplex crystallization behavior and mechanical properties of PLLA/PDLA blends. *Polymers (Basel)*. 2021;13(11):1851.

40. Margolis JM. *Engineering Thermoplastics: Properties and Applications*. CRC Press; 2020.

41. Luo F, Fortenberry A, Ren J, Qiang Z. Recent progress in enhancing poly (lactic acid) stereocomplex formation for material property improvement. *Front Chem*. 2020;8:688.

42. Giordano RA, Wu BM, Borland SW, Cima LG, Sachs EM, Cima MJ. Mechanical properties of dense polylactic acid structures fabricated by three dimensional printing. *J Biomater Sci Polym Ed*. 1997;8(1):63-75.

43. Gironi F, Frattari S, Piemonte V. PLA chemical recycling process optimization: PLA solubilization in organic solvents. *J Polym Environ*. 2016;24(4):328-333.

44. Leinster M. Things Pass By. Published online 1957.

45. Liu Z, Zhang M, Bhandari B, Wang Y. 3D printing: Printing precision and application in food sector. *Trends Food Sci Technol*. 2017;69:83-94.

46. Ellam R. 3D printing: you read it here first. *New Sci (1956)*. 2016;232(3099):52.

47. Bird J. Exploring the 3D printing opportunity. *The Financial Times Retrieved*. Published online 2012:8-30.

48. Kodama H. Background of my invention of 3D printer and its spread. *Patent Magazine of Japan Patent Attorneys Association*. 2014;67(13):109-118.

49. Kodama H. A scheme for three-dimensional display by automatic fabrication of three-dimensional model. *IEICE Trans on Electronics*. Published online 1981:237-241.

50. Barnatt C. *3D Printing: The Next Industrial Revolution*. ExplainingTheFuture.com; 2013. https://books.google.com.tr/books?id=Tvb6nAEACAAJ

51. Hoffman T. 3D printing: What you need to know. *PC Magazine*. Published online 2016:1-4.

52. Amon CH, Beuth JL, Weiss LE, Merz R, Prinz FB. Shape deposition manufacturing with microcasting: processing, thermal and mechanical issues. Published online 1998.

53. Miller A. The Evolution of 3D Printing: Past, Present and Future. *3D Printing Industry*. 2018;1.

54. Gregurić L. History of 3D printing: when was 3D printing invented. *Munich: All3DP*. Published online 2018.

55. McNaney T. Filabot: plastic filament maker. *Kickstarter, posted December*. 2011;19.

56. Grames E. 3D printer price: How much does a 3D printer cost in 2020. Published online 2020.

57. Frick L. How to smooth 3d-printed parts. *Machine Design*. Published online 2014.

58. Jacobs PF. *Rapid Prototyping & Manufacturing: Fundamentals of Stereolithography*. Society of Manufacturing Engineers; 1992.

59. Liu W, Zhou J, Ma Y, Wang J, Xu J. Fabrication of PLA filaments and its printable performance. In: *IOP Conference Series: Materials Science and Engineering*. Vol 275. IOP Publishing; 2017:012033.

60. Anycubic I3 Mega. https://www.anycubic.com/products/anycubic-i3-mega?_pos=7&_sid=cfc8ede01&_ss=r&variant=30084947345468

61. CONVENTIONAL MANUFACTURING VS 3D PRINTING. https://minifactory.fi. https://minifactory.fi/conventional-manufacturing-vs-3d-printing/

62. PLA vs. ABS: What are the differences? https://www.3dprintshed.com https://www.3dprintshed.com/blogs/news/pla-vs-abs-what-are-the-differences

63. IS THAT THE SOUND OF 3D PRINTED IP INFRINGEMENT? https://3dprintingindustry.com. https://3dprintingindustry.com/news/sound-3d-printed-ip-infringement-93851/

64. Filament Grinding. https://www.smith3d.com. https://www.smith3d.com/filament-grinding/

65. Torun AR, Yıldız EC, Dike AS, Sağlam İ, Choupani N. Fracture characterization and modeling of Gyroid filled 3D printed PLA structures . *Gruyter*. Published online 2021.

66. Farah S, Anderson DG, Langer R. Physical and mechanical properties of PLA, and their functions in widespread applications — A comprehensive review. *Adv Drug Deliv Rev*. 2016;107:367-392. doi:10.1016/j.addr.2016.06.012

67. Torun AR, Yıldız EC, Kaya ŞH, Choupani N. Mixed-mode fracture behavior of 3D-printed PLA with zigzag filling. *Green Mater*. 2020;9(1):29-36. doi:10.1680/jgrma.20.00013

68. Young Modulus. Accessed November 12, 2022. https://depts.washington.edu/matseed/mse_resources/Webpage/Biomaterials/young%27s_modulus.htm

69. Leading technology for biobased PLA plastics. sulzer.com. https://www.sulzer.com/en/shared/stories/leading-technology-for-biobased-pla-plastics

70. https://tr.wikipedia.org. Enantiyomer. https://tr.wikipedia.org/wiki/Enantiyomer

71. Zolfagharian A, Khosravani MR, Kaynak A. Fracture resistance analysis of 3D-printed polymers. *Polymers (Basel)*. 2020;12(2). doi:10.3390/polym12020302

72. Hossein Abadi R, Refah Torun A, Mohammadali Zadeh Fard A, Choupani N. Fracture characteristics of mixed-mode toughness of dissimilar adherends (cohesive and interfacial fracture). *J Adhes Sci Technol*. 2020;34(6):599-615. doi:10.1080/01694243.2019.1674102

73. Savioli Lopes M, Jardini AL, Maciel Filho R. Poly (lactic acid) production for tissue engineering applications. In: *Procedia Engineering*. Vol 42. Elsevier Ltd; 2012:1402-1413. doi:10.1016/j.proeng.2012.07.534

74. Michalski A, Brzezinski M, Lapienis G, Biela T. Star-shaped and branched polylactides: Synthesis, characterization, and properties. *Prog Polym Sci*. 2019;89:159-212. doi:10.1016/j.progpolymsci.2018.10.004

75. Wang Q, Li Y, Zhou X, et al. Toughened poly(lactic acid)/BEP composites with good biodegradability and cytocompatibility. *Polymers (Basel)*. 2019;11(9). doi:10.3390/polym11091413

76. Shameli M, Choupani N. Fracture Criterion of Woven Glass-Epoxy Composite Using a New Modified Mixed-Mode Loading Fixture. *Int J Appl Mech*. 2016;8(2). doi:10.1142/S1758825116500150

77. Rountree CL, Kalia RK, Lidorikis E, Nakano A, van Brutzel L, Vashishta P. Atomistic aspects of crack propagation in brittle materials: Multimillion atom molecular dynamics simulations. *Annual Review of Materials Science*. 2002;32:377-400. doi: 10.1146/annurev.matsci.32.111201.142017

78. Ribeaucourt R, Baietto-Dubourg MC, Gravouil A, Berthier Y. A mixed mode fatigue crack model with the coupled X-FEM/LATIN method. Application to rolling contact fatigue (RCF). *Tribology and Interface Engineering Series*. 2005;48:329-341. doi:10.1016/s0167-8922(05)80035-5

79. B.S Majumdar, D. Hunston. *Continuous Parallel Fiber Composites: Fracture*.

80. Park SJ, Seo MK. *Solid-Solid Interfaces*. Vol 18.; 2011. doi:10.1016/B978-0-12-375049-5.00004-9

81. Shimadzu . Accessed November 30, 2022. https://www.shimadzu.eu

82. Taylor D. *Geometrical Effects in Fatigue: A Unifying Theoretical Model*. Vol 21.; 1999.

83. Courtin S, Gardin C, Bézine G, Hamouda HBH. Advantages of the J-integral approach for calculating stress intensity factors when using the commercial finite element software ABAQUS. *Eng Fract Mech*. 2005;72(14):2174-2185. doi: 10.1016/j.engfracmech.2005.02.003

84. Zhu XK. *Numerical Determination of Stress Intensity Factors Using ABAQUS*.; 2014. http://www.asme.org/about-asme/terms-of-use

85. Broberg KB. *CRITICAL REVIEW OF SOME THEORIES IN FRACTURE MECHANICS*.

86. Blandford GE, Ingraffeas AR, Liggett JA. *TWO-DIMENSIONAL STRESS INTENSITY FACTOR COMPUTATIONS USING THE BOUNDARY ELEMENT METHOD*. Vol 17.; 1981.

87. Moreira PMGP, Pastrama SD, de Castro PMST. Three-dimensional stress intensity factor calibration for a stiffened cracked plate. *Eng Fract Mech*. 2009;76(14):2298-2308. doi: 10.1016/j.engfracmech.2009.07.003

88. Jia ZH, Shippy DJ, Rizzo FJ. *O N THE COMPUTATION OF TWO-DIMENSIONAL STRESS INTENSITY FACTORS USING THE BOUNDARY ELEMENT METHOD*. Vol 26.

89. Letcher T, Waytashek M. *MATERIAL PROPERTY TESTING OF 3D-PRINTED SPECIMEN IN PLA ON AN ENTRY-LEVEL 3D PRINTER*.; 2014. http://www.asme.org/about-asme/terms-of-use

90. Raj Sa. *A Case Study of 3D Printed PLA and Its Mechanical Properties*. Vol 5.; 2018. www.sciencedirect.comwww.materialstoday.com/proceedings

91. Anand Kumar S, Shivraj Narayan Y. Tensile testing and evaluation of 3D-printed PLA specimens as per ASTM D638 type IV standard. In: *Lecture Notes in Mechanical Engineering*. Pleiades journals; 2019:79-95. doi:10.1007/978-981-13-2718-6_9

CURRICULUM VITAE